ORIGINAL PAPER

Effect of water saturation on the strength of sandstones: experimental investigation and statistical analysis

Shibing Huang[1,2] · Shilin Yu[1]

Abstract

Sandstones are widespread on the earth and are often damaged by water. Although there is a consensus that the strength of sandstones will decrease when they are in contact with water, the intrinsic properties controlling the water-weakening mechanism of sandstones are not completely clear. In this study, the uniaxial compression strength (UCS), point load index (PLI), and Brazilian tensile strength (BTS) of four clay-bearing sandstones with water saturation from 0 to 100% were measured by experiments. The results showed that a remarkable strength loss occurred when the water saturation increased from 0 to 60% ∼ 80%, and then, the reduction rate slowed dramatically. Therefore, the critical water saturation level at which considerable strength loss due to the water-weakening effect is produced is 60 ∼ 80%. In addition, the strength loss law caused by increasing water saturation satisfied both the exponential decay function and logarithmic decay function. The multiple linear regression method was used to model the relationship between the intrinsic properties and UCS loss caused by water-weakening effects considering the effect of water saturation. The porosity, elastic modulus and clay mineral content were automatically selected by the best subset regression as the main intrinsic properties controlling the water-weakening degree of sandstones. In addition, the critical water saturation level and the role that clay minerals play in the water-weakening effects of sandstones were comprehensively discussed. This study contributes to a better understanding of the water-weakening mechanism and provides a better strength estimation model for sandstones with different water saturation levels.

Keywords Water saturation · Strength loss · Water weakening · Clay-bearing sandstone · Strength estimation model

Abbreviations

σ_c	Uniaxial compressive strength
σ_c^D, σ_c^S	Uniaxial compressive strength for dry and saturated sandstones, respectively
σ_t	Tensile strength
σ_t^D, σ_t^S	Tensile strength for dry and saturated sandstones, respectively
$I_{s(50)}$	Point load strength index of the specimen with diameter of 50 mm
$I_{s(50)}^D$, $I_{s(50)}^S$	Point load strength indexes for dry and saturated sandstones, respectively
W_a	Water content, the mass ratio of water to dry rock
CM	Content of clay minerals
n	Number of samples
V_s	The volume of rock
m_1, m_2	Mass of dry, forced saturated rocks, respectively
$m_3(t)$	Unforced water absorption content after immersing in water for time t
V_{pd}, V_{ps}	P-wave velocity for dry and saturated sandstones, respectively
S_r	Saturation degree of rocks, the volume ratio of water to total pores
S_{rc}	Critical saturation degree of rocks
E	Elastic modulus of rocks
E_d, E_s	Elastic modulus of dry and saturated rocks, respectively
ρ_d, ρ_w	Density of dry rocks and liquid water, respectively

✉ Shibing Huang
huangshibing@wust.edu.cn

Shilin Yu
1035200909@qq.com

1 School of Resources and Environmental Engineering, Wuhan University of Science and Technology, Wuhan, China

2 Hubei Key Laboratory for Efficient Utilization and Agglomeration of Metallurgic Mineral Resources, Wuhan, China

W_n W_f	Water absorption ratio at natural and forced vacuum conditions, respectively
LF	The UCS loss fraction
A, B and C	Material parameters
R^2, R^2	The adjusted and original determination coefficients, respectively
m, p	The sample size and number of independent variables, respectively
β_0, β_1, β_2 and β_3	The residual sum of square error
RSS_p	The residual sum of square error
$\hat{\sigma}^2$	Mean square error

Introduction

The rocks used in engineering inevitably encounter water, for example, tropical rock slopes, stone buildings and water-rich rock tunnels. In addition, some rock engineering structures may be continuously immersed in water, such as rock reservoir slopes, rock diversion tunnels, dam bedrocks and so on. When the structures are contacted by water, the water will enter voids and thus cause the rocks to experience strength loss and stiffness reduction (Chen et al. 2019; Huang et al. 2022b). Sandstones, as typical sedimentary rocks, are widely distributed on the earth and are often encountered in rock engineering. In addition, they are widely used as construction materials because of their good cementation ability and availability (Sun and Zhang 2019). Most sandstones contain some clay minerals, which are very sensitive to water. However, the influence of water saturation on clay-bearing sandstones and the main intrinsic properties controlling the water-weakening effect of sandstones are not completely understood.

In recent decades, many scholars have focused on the strength loss of sandstones from completely dry to saturated conditions (Erguler and Ulusay 2009; Wasantha and Ranjith 2014; Kim and Changani 2016; Wasantha et al. 2018). Hawkins and McConnell (1992) measured the UCS of 35 British sandstones with different water content levels. They found that the maximum uniaxial compressive strength (UCS) loss of sandstones exceeded 70% under completely saturated conditions. Vásárhelyi (2003) proposed that the relationship between the saturated UCS and dry UCS satisfied a linear function, and the mean UCS loss was approximately 24.1% after complete saturation by further analysing the experimental data from Hawkins and McConnell (1992). Most rocks are unsaturated in the natural absorption process, and a low water content level in rocks can cause a great strength loss. Vásárhelyi and Ván (2006) claimed that the strength of some sandstones had a remarkable reduction with only 1% water saturation. Cherblanc et al. (2016) observed that more than 90% strength loss occurred even in a natural absorption condition with a 97% RH atmosphere. Liu et al. (2020) proposed that

more than 90% of the UCS loss occurred below 60% water saturation for clay-bearing red sandstones. Therefore, the water content is an important factor influencing the strength of sandstones even at low water saturation levels.

Although there is a basic consensus from scholars that the strength of rocks decreases with increasing water saturation, the main intrinsic properties controlling water-weakening effects are still not clear. Generally, the effect of water saturation on sandstone includes chemical erosion and physical softening (Kim and Changani 2016). Chemical erosion is caused by the solution or dispersion of clay minerals between mineral grains, and it is highly relevant to the clay mineral content (Cherblanc et al. 2016). Many studies have concluded that the effect of dry–wet cycles on the strength and P-wave velocity of sandstones in water is very small when the sandstone does not contain clay minerals or expansible clay minerals are absent (Sun and Zhang 2019; Huang et al. 2021b). This illustrated that the physical softening, including the reduction of friction and fracture energy, should be responsible for the strength loss of sandstones in contact with water if the sandstones contain few clay minerals (Zhao et al. 2017). The presence of water could dissolve the cemented minerals around hard particles and increases the distance between particles thus reduce the friction between them (Chen et al. 2017; Li et al. 2021; Huang et al. 2022c). In addition, water could also lower the surface free energy and then cause a reduction in the strength of the rocks (Zhao et al. 2017). He et al. (2019) claimed that a high clay content in sandstones did not always lead to a low strength but would cause a high strength loss when in contact with water. Wasantha et al. (2018) held that sandstones with more clay minerals were more greatly weakened by water than those with more quartz. Ruedrich et al. (2011) proposed that clay minerals had small pores but high moisture swelling, and an expansion pressure would be produced when absorbing water, which influenced the water softening of sandstones. Above all, the type and proportion of clay minerals were crucial intrinsic factors influencing the water-weakening degree of sandstones. In addition, there may be some other factors influencing the strength of sandstones, such as the porosity, elastic modulus, and water absorption capability (Palchik 1999; Kim et al. 2017; Yu et al. 2019). A sandstone with a large porosity has a relatively smaller strength, but it will absorb more water quickly, which may cause a rapid decrease in the strength.

In addition to the influencing factors, a proper strength estimation function is also essential to predict the strength loss of sandstones after absorbing water. Three typical empirical equations have been proposed to estimate the strength loss of rocks with different water saturations, including exponential functions (Hawkins and McConnell 1992; Masoumi et al. 2017), logarithmic functions (Huang et al. 2020a, 2021b) and polynomial functions (Tang 2018).

However, these empirical functions have only been used for a few rock types and limited experimental data are available to date. The empirical function that is most suitable to estimate the strength loss caused by water saturation remains unclear. In addition, the unknown parameters in these functions need to be determined by fitting the experimental data, which is laborious and time-consuming.

In this study, the UCS, BTS and PLI of four sandstones with different water saturation levels (0 ~ 100%) were measured to find the most competitive strength estimation function against water saturation. Then, the main physico-mechanical properties that played major roles in the water-weakening process of sandstones were determined by using the best subset regression method. A model to determine the quantitative relationship between the critical physico-mechanical properties and the unknown parameter in the UCS estimation equation was built. The main novelty of this paper may be that the strength loss law of sandstones with increasing water saturation levels and the intrinsic physico-mechanical properties controlling the water-weakening effects were completely determined by a combination of experimental and statistical analysis methods. This paper can provide a better understanding of the water-weakening mechanism of sandstones.

Experimental procedures

Preparation of the rock samples

Four sandstones (grey, red, brown and yellow) were used to investigate the influence of water saturation on strength. Red sandstones were collected from Yichang, Hubei Province. The other sandstones were collected from Zigong, Sichuan Province. There are approximately 72 standard cylindrical samples (diameter = 50 mm and height = 100 mm) used to measure the uniaxial compressive strength (UCS). These 72 standard sandstones were divided into six groups with different water saturation levels, including 0%, 30%, 60%, 80%, 90% and 100%. Eighty-four flat cylindrical samples (diameter = 50 mm and height = 30 mm) were used to measure the Brazilian tensile strength (BTS), and the other 84 flat cylindrical samples (diameter = 50 mm and height = 30 mm) were used to measure the point load strength index (PLI). Seven different saturation groups were set for the BTS and PLI tests, including 0%, 10%, 30%, 60%, 80%, 90% and 100%. Therefore, each group has three parallel experiments to avoid the error caused by the discreteness of the samples. The preparation process of these rock samples is in accordance with the method suggested by ASTM (2008b). All the rock samples were taken from the same block by using a drilling machine with a hollow bit (internal diameter = 50 mm). Then, they were cut into a specified length by using a rock cutting machine. Both ends of the sample were polished parallel to each other and perpendicular to the axial direction using a grinding machine. The flatness error of the surfaces should be less than 0.025 mm. The designed water saturation level was ensured by natural dehydration in an air-conditioned room after forced vacuum saturation, which was introduced in detail in our previous literature (Liu et al. 2020). There is no need to restate the process of preparing the different water saturation levels here, but it should be noted that the water saturation error percentage was less than 0.5% according to a high-accuracy electronic balance with a precision of 0.01 g. All the samples were wrapped with plastic films after reaching the assigned saturation level to prevent water loss. The process for preparing the sandstone samples is shown in Fig. 1.

Petrographic analysis

Several slices were cut from the fresh sandstone and ground into powder using an angle grinder (< 45 µm) (Fig. 1). The powder was dried in a heating oven at 105 °C, and then, it was used to measure the mineral component by using TTRIII X-ray diffraction (XRD). The "K value" method suggested in SY/T 5163–2018 (China Standard 2018) was adopted to make a quantitative analysis of the mineral components (Zeng et al. 2010). To investigate the mineral particle structure and their contact state, a 3D colour optical microscope (Keyence, VHX-5000) was used to magnify the sandstone samples to capture their surface profiles.

Physico-mechanical tests

The UCS, BTS and PLI tests were carried out in accordance with the methods suggested by ASTM (2010, 2008a and 2008c), respectively. UCS tests were performed on an electrohydraulic servo mechanical machine (WAW-300) with a loading rate of 0.24 mm/min. The BTS, also called the splitting tensile strength, was tested on a microcomputer control electronic universal testing machine (WDW-100) with a loading rate of 0.12 mm/min. A wedge indenter was added between the cylindrical sample and loading plane to ensure a diametral line compression condition. PLI was tested by using a manual point load tester under a constant loading rate (Fig. 2a).

The porosity was tested using the vacuum saturation method. First, standard cylindrical samples were dried at 105 °C for 24 h. The dry masses of these samples were tested by using a high-accuracy electronic balance with a precision of 0.01 g. Then, these dry samples were placed into a vacuum container at −0.1 MPa to remove the air from the pores. Liquid water was injected into this container, and these samples absorbed water for 48 h at −0.1 MPa. After that, completely saturated samples could be derived, and their masses were

Fig. 1 Preparation procedure of cylindrical sandstone samples and powder

measured again using an electronic balance. As a result, the porosity could be calculated by using the difference in mass values of the saturated and dry samples. The unforced or natural water absorption process was measured by immersing a whole dry sample into pure water at one atmospheric pressure of 101 kPa (Fig. 2b). The physico-mechanical test process and devices are plotted in Fig. 2.

Experimental results

### Petrographic characteristics

The mineral compositions of these sandstones were quantified by XRD (Fig. 3). The XRD results show that the total clay mineral contents are 21.1%, 10.6%, 4.6% and 7.0% for the grey, red, brown and yellow sandstones, respectively.

Enlarged surface profiles of the mineral particles are plotted in Fig. 4. The maximum mineral diameters of quartz are approximately 200 μm, 400 μm, 300 μm and 300 μm for the grey, red, brown and yellow sandstones, respectively. The minimum mineral diameters are less than 200 μm. The feldspar contents are approximately 10.4%, 21.7% and 64.6% in the grey, red and yellow sandstones, respectively. However, in brown sandstones, the quartz fraction is 95.4%, but feldspar is absent. By petrographic analysis, it can be concluded that grey sandstone is a type of fine-grained lithic sandstone, red and yellow sandstones belong to medium-fine-grained arkosic sandstones, and brown sandstone is a type of medium-fine-grained quartzose sandstone. The hard particles (quartz and feldspar) of these sandstones are well cemented by soft minerals, such as clay minerals. Therefore, they are also typical clay-bearing sandstones. The basic physical properties of these sandstones are given in Table 1.

Fig. 2 Main physico-mechanical tests and related equipment. **a** Mechanical strength test procedure and equipment. **b** Forced saturation and natural water absorption process
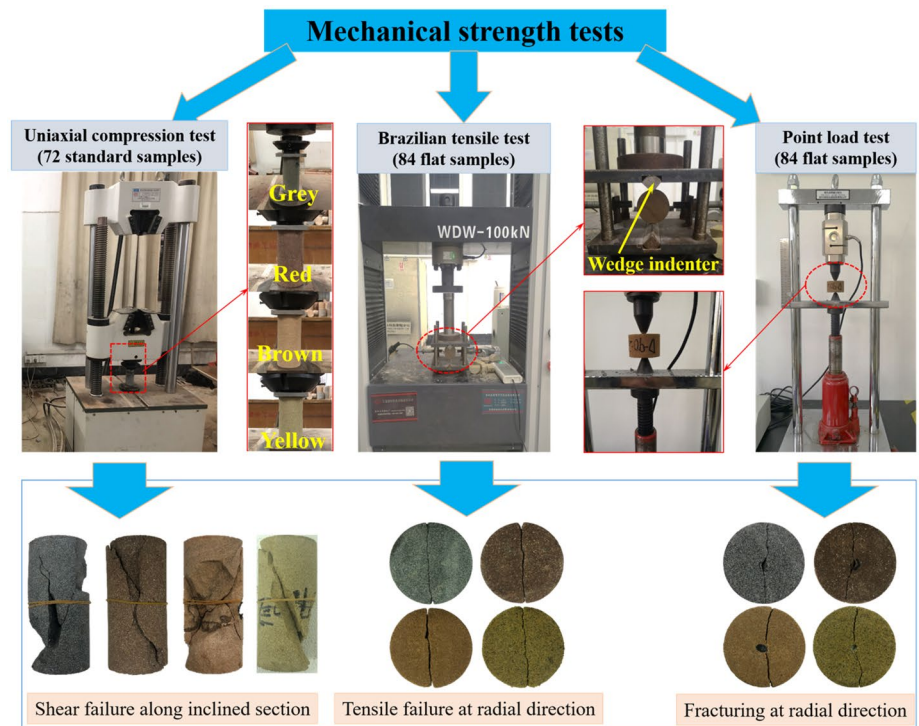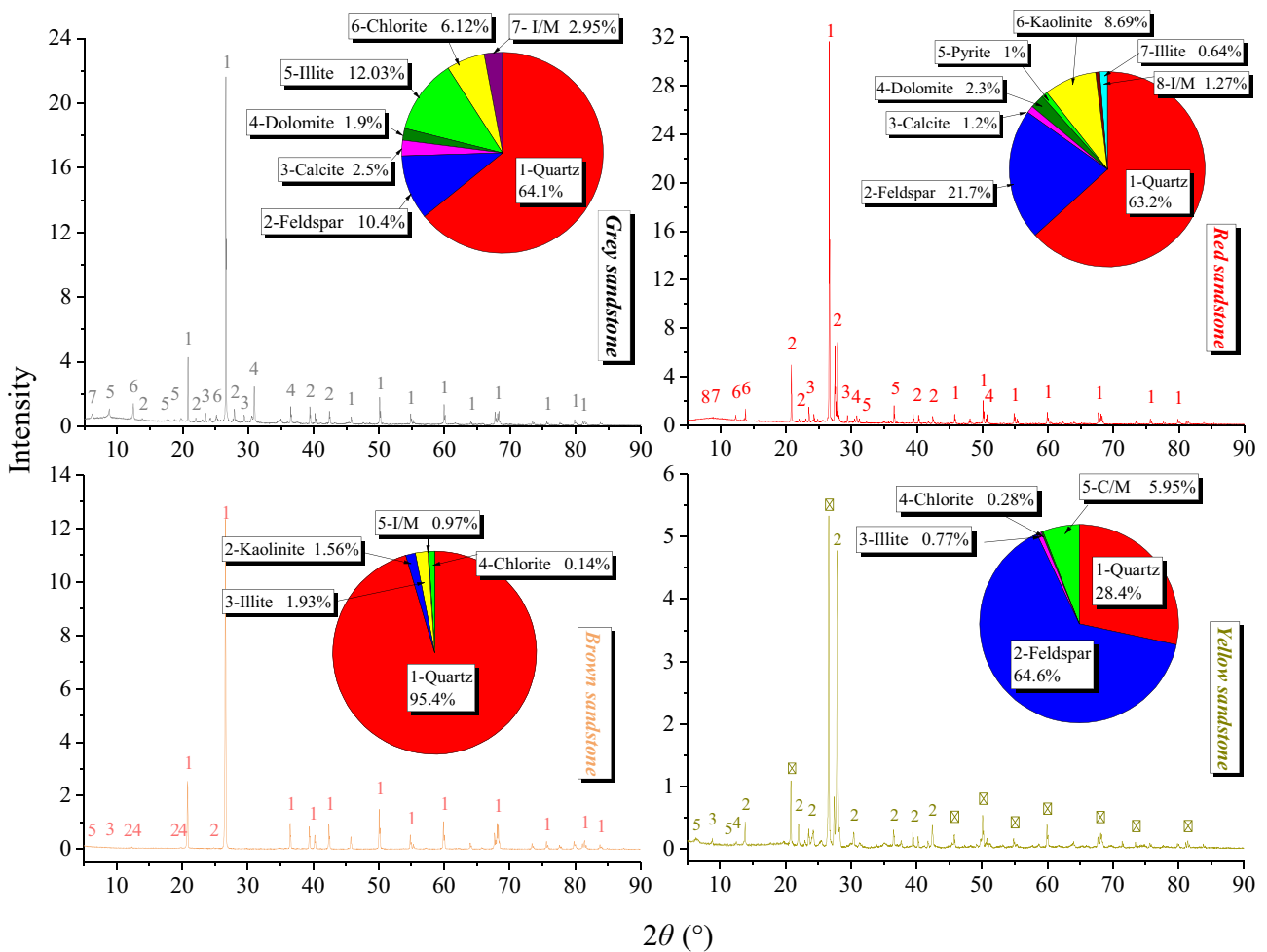

(a)
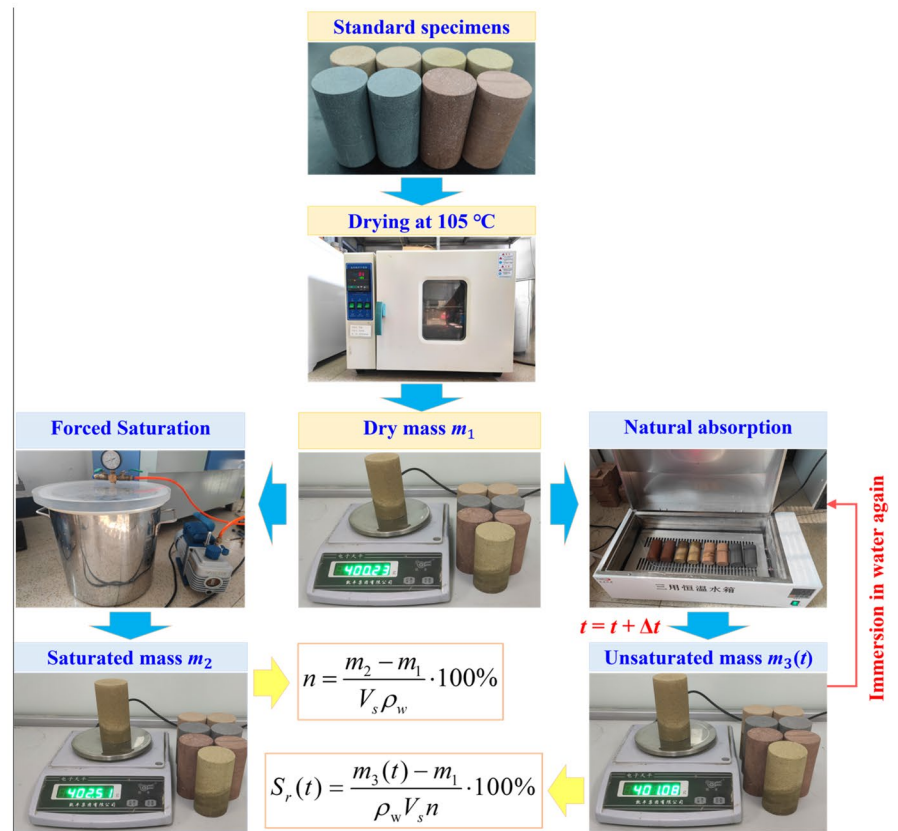
(b)

Fig. 3 X-ray diffraction pattern of these four sandstones

Water absorption process

Figure 5 shows that the absorbed water content increases very quickly in several minutes when immersed in water under natural conditions (101 kPa, 20 °C). Then, the water content reaches a constant level after several hours. The natural absorption water content by weight for yellow sandstone is approximately 7.72%, while it is only 1.5% for the grey sandstone at the final stable state. The water content increases with increasing porosity and is a typical exponential function of the soaking time. A novel finding is that the natural absorption saturation level is 70~85%, which is relatively stable compared with the water absorption content. Therefore, the water saturation S_r is used in this study instead of the water content W_a to determine the critical water saturation level for which a remarkable reduction of strength occurs.

UCS

The UCS of sandstones has a significant reduction with increasing water saturation, as shown in Fig. 6. However, most of the UCS loss occurs when the water saturation increases from 0 to 60%. Beyond 80% water saturation, the reduction rate of the UCS decreases substantially. Several typical decay functions have been proposed to estimate the UCS loss of sandstones caused by water saturation, including polynomial functions (Tang 2018), logarithmic functions (Huang et al. 2020a, 2021b) and exponential functions (Hawkins and McConnell 1992; Shi et al. 2016), which can be written as follows:
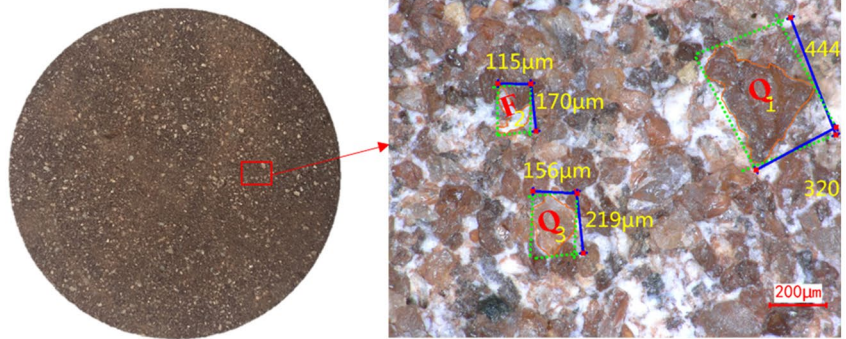
$$\text{Polynomial function}: \sigma_c = C + B \cdot S_r + A \cdot S_r^2 \tag{1}$$

$$\text{Logarithmic function}: \sigma_c = C - B \cdot \log\left(A \cdot S_r + 1\right) \tag{2}$$
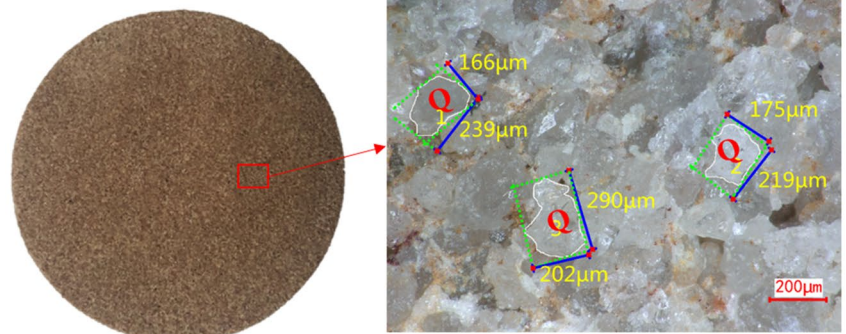
Fig. 4 Enlarged apparent structure of sandstones (original magnification 200×). **a** Grey sandstone. **b** Red sandstone. **c** Brown sandstone. **d** Yellow sandstone
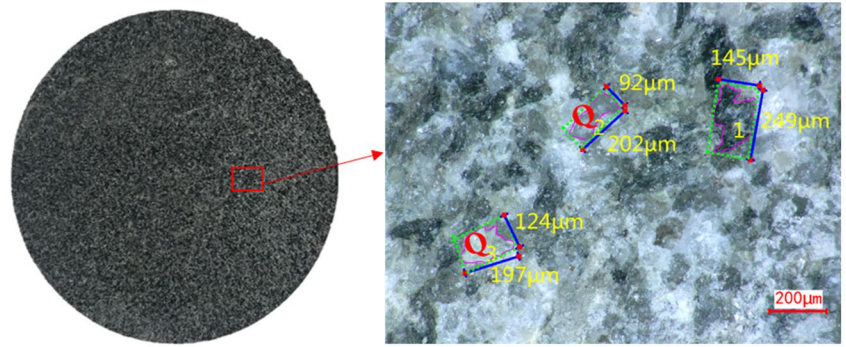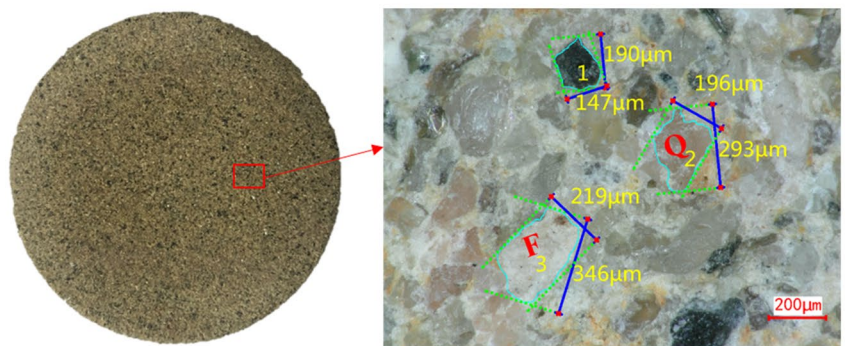

(a)

(b)

(c)

(d)

Table 1 The basic physical properties of these four sandstones

Type	ρ_d (g/cm^3)	n (%)	Water absorption content (%)		P-wave velocity (m/s)		CM (%)
			W_n	W_f	V_{pd}	V_{ps}	
Grey	2.57	4.53	1.50	1.76	2845	3178	21.1
Red	2.40	9.95	2.90	4.12	2918	3246	10.6
Brown	2.26	14.81	4.62	6.56	1381	1701	4.6
Yellow	2.10	21.78	7.72	10.39	1702	2089	7.0

Exponential function : $\sigma_c = C + B \cdot e^{-A \cdot S_r}$ (3)

where σ_c is the uniaxial compression strength. S_r is the water saturation degree. A, B and C are the material parameters that need to be determined by experimental means.

Generally, UCSs of the completely dry and saturated sandstones are easy to measure. To reduce the undetermined parameters, substituting the UCS values at the dry and saturated conditions into Eqs. (1) ~ (3) yields the following:

Polynomial function : $\sigma_c = A \cdot S_r^2 + (\sigma_c^S - \sigma_c^D - A)S_r + \sigma_c^D$ (4)

Logarithmic function : $\sigma_c = \dfrac{\sigma_c^S - \sigma_c^D}{\log(1 + A)}(1 + A \cdot S_r) + \sigma_c^D$ (5)

Exponential function : $\sigma_c = \dfrac{\sigma_c^D - \sigma_c^S}{1 - e^{-A}}\left(e^{-A \cdot S_r} - 1\right) + \sigma_c^D$ (6)

where σ_c^D and σ_c^S are the uniaxial compressive strengths for dry and saturated sandstones, respectively.
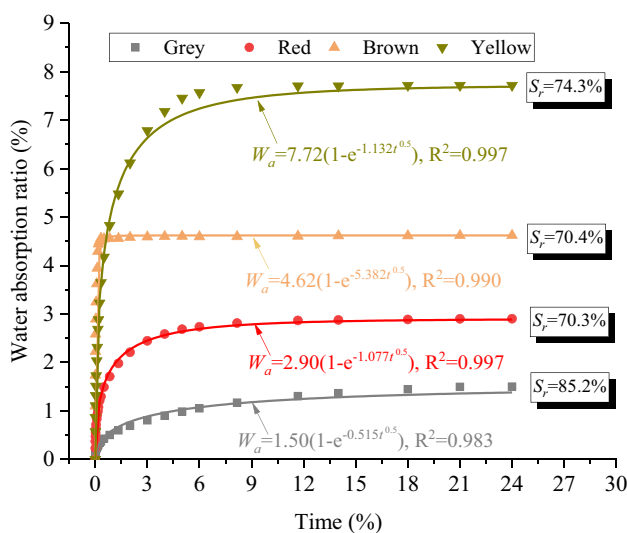
Finally, only one undetermined parameter, i.e., A, is preserved in Eqs. (4) ~ (6). Figure 6 shows that both the exponential function and logarithmic function can be used to describe the loss law of UCS against water saturations well. The polynomial function may be not monotonic when the water saturation increases from 0 to 100%; therefore, using a polynomial function is not suggested here. For example, the UCS of the yellow sandstone continually decreases with increasing water saturation; however, the calculated values of UCS using a polynomial function first decrease and then exhibit an abnormal increasing trend beyond 80% water saturation (Fig. 6d). In this study, the exponential function is used to predict the strength loss caused by increasing water saturation because it can better reflect the steady state of the UCS at a high water saturation level, and it is more commonly used in the previous literature. Both the UCS and the elastic modulus satisfy the exponential decay function (Figs. 7 and 8). This illustrates that the sandstones become weak and soft in the presence of water. The UCS decreases quickly when the water saturation increases from 0 to 80%, and then, the UCS values of these sandstones are almost constant beyond 80% water saturation, except for the brown sandstone, which contains some rock veins. The existence of these rock veins may have some influence on the water-weakening law of the brown sandstone.
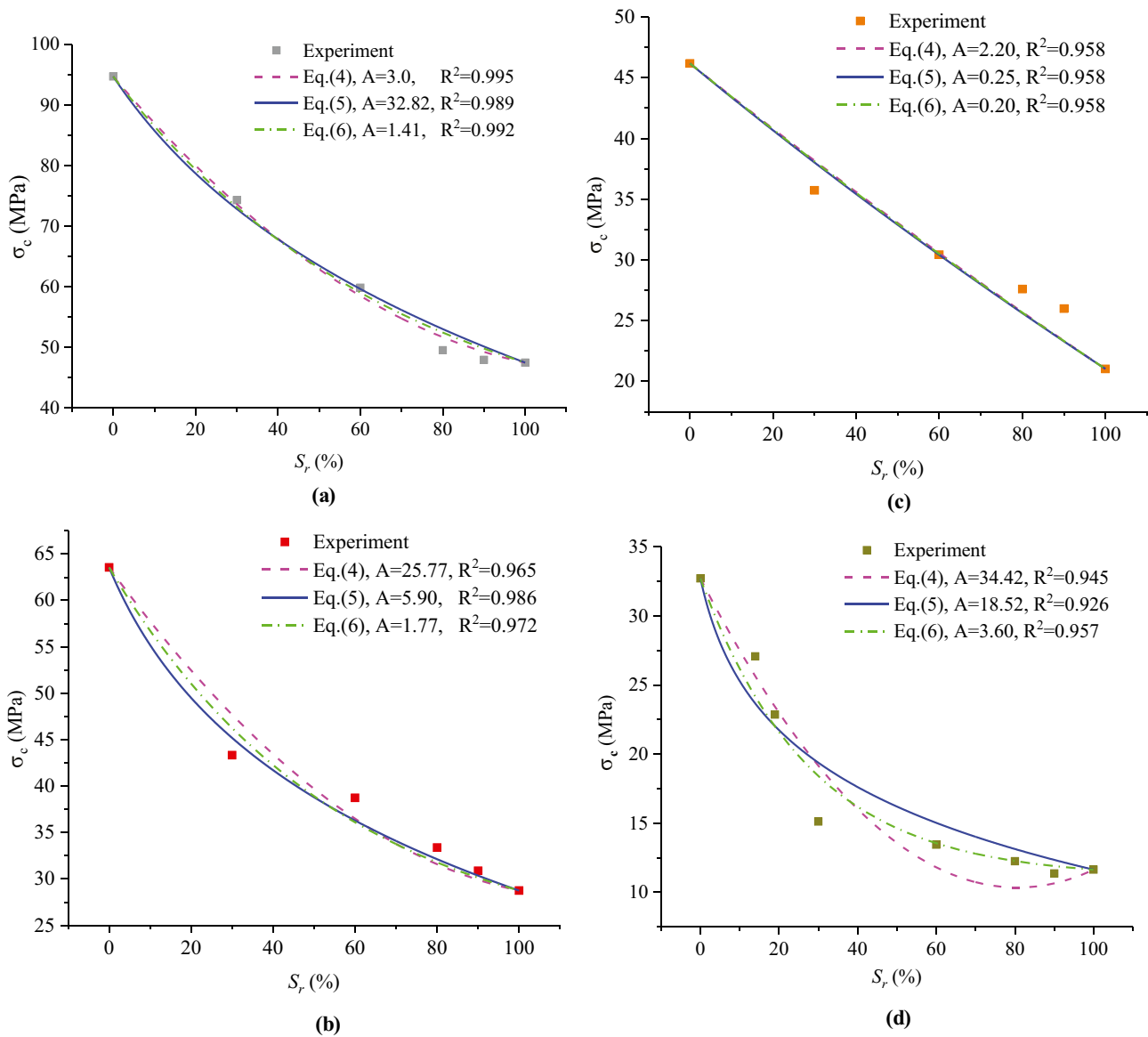
BTS and PLI

Both the BTS and PLI decrease with increasing water saturation levels. The BTS and PLI may also be expressed as exponential functions of the water saturation by referring to the change law of UCS, as follows (Figs. 9 and 10):

$$\sigma_t = \frac{\sigma_t^D - \sigma_t^S}{1 - e^{-A}}(e^{-A \cdot S_r} - 1) + \sigma_t^D \tag{7}$$

$$I_{s(50)} = \frac{I_{s(50)}^D - I_{s(50)}^S}{1 - e^{-A}}(e^{-A \cdot S_r} - 1) + I_{s(50)}^D \tag{8}$$

where σ_t is the Brazilian tensile strength. σ_t^D and σ_t^S are the Brazilian tensile strengths of dry and saturated sandstones, respectively. $I_{s(50)}$ is the point load strength index of the specimen with a diameter of 50 mm. $I_{s(50)}^D$ and $I_{s(50)}^S$ are the

Fig. 5 Water absorption process of sandstone samples during natural immersion

Fig. 6 Comparison of three UCS estimation functions against water saturations. **a** Grey sandstone. **b** Red sandstone. **c** Brown sandstone. **d** Yellow sandstone

point load strength indexes of dry and saturated sandstones, respectively.

The BTS and PLI values of these sandstones also decrease more quickly at low water saturations, especially when the water saturation is less than 60%. When the water saturation increases from 0 to 60%, the BTS values decrease by 41.7%, 56.4%, 38.3% and 61.3% for the grey, red, brown and yellow sandstones, respectively. As the water saturation continues to increase from 60 to 100%, the BTS values decrease by 57.8%, 55.7%, 49.8% and 75% for the grey, red, brown and yellow sandstones, respectively. Therefore, the corresponding loss ratios of BTS at 60% water saturation to the total BTS loss at 100% water saturation are 72.1%,

100%, 76.9% and 81.7% for grey, red, brown and yellow sandstones, respectively. In addition, the PLI loss at 60% water saturation occupies 82.7%, 86.3%, 61.9% and 96% of the total PLI loss at 100% water saturation for the grey, red, brown and yellow sandstones, respectively. It can be concluded that 60% water saturation can cause a considerable reduction in strength. The natural water saturation levels of these four sandstones range from 70.3 to 85.2% (Fig. 5); therefore, sandstones under natural immersion conditions will suffer most of the water-weakening action and strength loss. Therefore, more attention should be given to the water-weakening process of engineering rocks in the field when water is available, such as on rainy days.
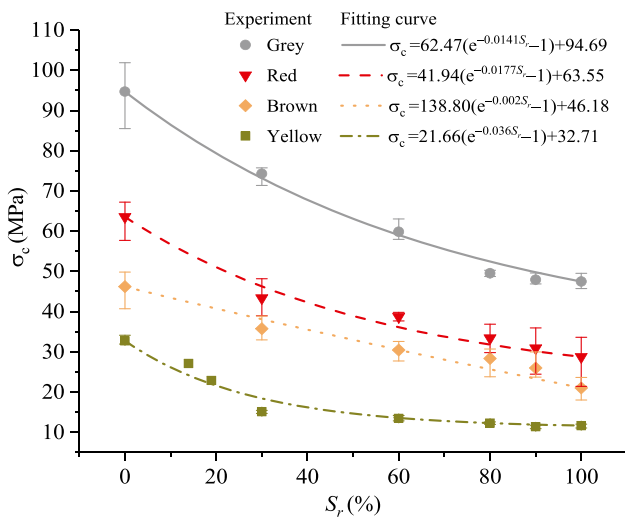
Fig. 7 Change of UCS against the water saturation

Correlation of the UCS and BTS with PLI

PLI is often used to estimate the UCS and BTS (Kahraman and Gunaydin 2009; Heidari et al. 2012) because PLI is easy to measure in the field using only a small point load tester. The correlation of the UCS and BTS with PLI for these four sandstones can be obtained by linear fitting (Fig. 11), which can be expressed as follows:

$$\sigma_c = 20.5 I_{s(50)} \tag{9}$$

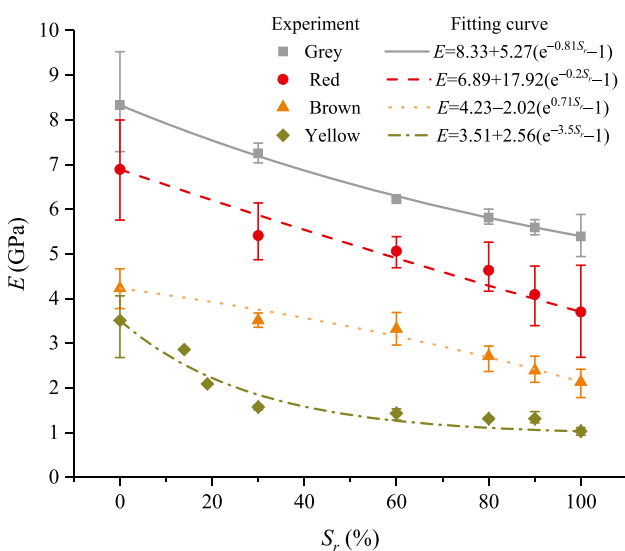$$\sigma_t = 1.32 I_{s(50)} \tag{10}$$

Fig. 8 Change of elastic modulus against the water saturation

The determination coefficients are 0.94 and 0.99 by using Eqs. (9) and (10), respectively. This result illustrates that although the sandstones contain different water saturation levels, the linear relationships are very good with high determination coefficients. Therefore, PLI is suitable to estimate the UCS and BTS of sandstones regardless of the water saturation level. Equation (9) is very similar to the relation suggested by the International Society for Rock Mechanics (ISRM), in which the linear coefficient range is from 20 to 25 (ISRM 1985).

A developed prediction model of UCS considering water saturation levels

In Eq. (6), there is one material parameter, i.e., A, that must be determined to estimate the UCS of sandstones containing different water saturation levels. If the UCS values of sandstones containing different water saturation levels are measured by experiment, the value of A can be determined by fitting the experimental data using Eq. (6). However, mechanical tests are laborious and time-consuming. The UCS loss of sandstones caused by water saturation can be determined using several easily available initial physico-mechanical parameters. To build the relationship between A and the initial physico-mechanical properties, more experimental data were collected from the previous literature to perform statistical analysis (Fig. 12). Multiple linear regression based on 22 types of sandstones was conducted with the aid of statistical software, such as Minitab and Excel. The basic physico-mechanical properties of these sandstones are given in Table 2. The best parameter subsets and optimal multiple linear regression are selected by using the adjusted R-squared ($\hat{R}^2$) and the value of Mallows' C_P. The best fit will have the highest $\hat{R}^2$ value but the lowest C_P value.

The adjusted $\hat{R}^2$ is used to eliminate the effect of the independent variable number as follows:

$$\hat{R}^2 = 1 - (1 - R^2) \times \frac{m - 1}{m - p - 1} \tag{11}$$

where $\hat{R}^2$ and R^2 are the adjusted and original determination coefficients, respectively. m and p are the size of samples and number of independent variables, respectively.

C_p is defined as a criterion to assess fits when models with a different number of parameters are being compared. It is defined as follows:

$$C_p = \frac{RSS_p}{\hat{\sigma}^2} + (2p - n) \tag{12}$$

where RSS_p represents the residual sum of the square error for a model with p independent variables, and $\hat{\sigma}^2$ denotes the mean square error based on the full model.
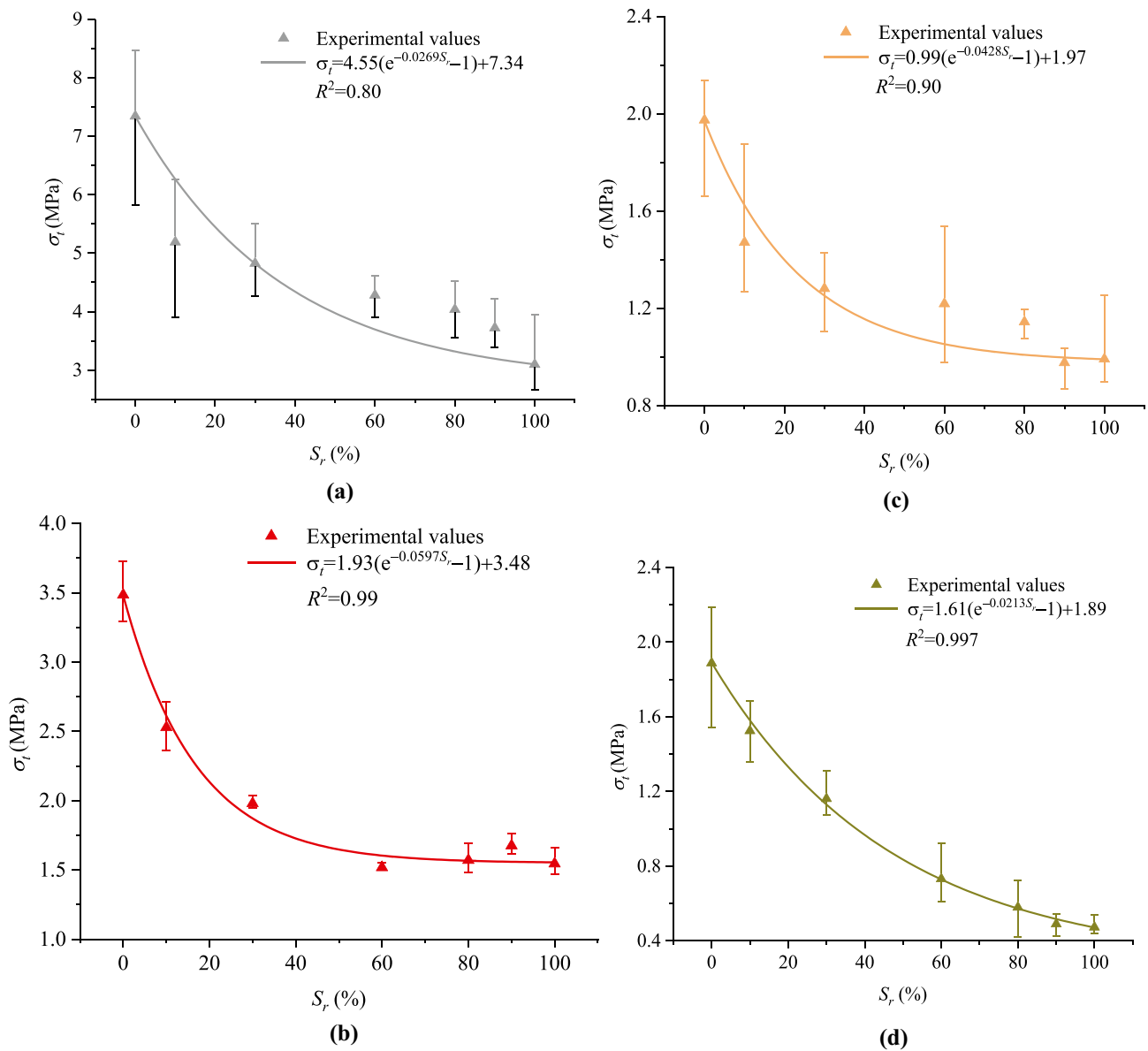
Fig. 9 The influence of water saturations on the BTS of sandstones. **a** Grey sandstone. **b** Red sandstone. **c** Brown sandstone. **d** Yellow sandstone

The $\hat{R^2}$ and C_p values calculated from different parameter sets are given in Table 3. This illustrates that the optimal multiple linear regression model can be expressed as follows:

$$A = \beta_0 + \beta_1 \times n + \beta_2 \times E_s + \beta_3 \times CM \tag{13}$$

where β_0, β_1, β_2 and β_3 are the coefficients, which are derived from the best subset regression (Table 4).

The final estimation function of UCS for the sandstones containing any water saturation can be expressed as follows:

$$\sigma_c = \frac{\sigma_c^D - \sigma_c^S}{1 - e^{-A}}(e^{-A \cdot S_r} - 1) + \sigma_c^D \tag{14}$$

where

$$A = -0.743 + 0.1268n(\%) + 0.1358E_s(\text{GPa}) + 0.0489CM(\%) \tag{15}$$

The predicted values of A are plotted against the measured results in Fig. 13, which shows good consistency. The value of A varies from 1 to 7 for these 22 sandstones. From Eq. (15), it can be concluded that the value of A is proportional to the porosity, elastic modulus and clay mineral content. The UCS values of sandstones decrease more quickly at low saturation levels for larger A values; therefore, clay-bearing sandstones with high porosity, large clay mineral content and large elastic modulus values are more sensitive
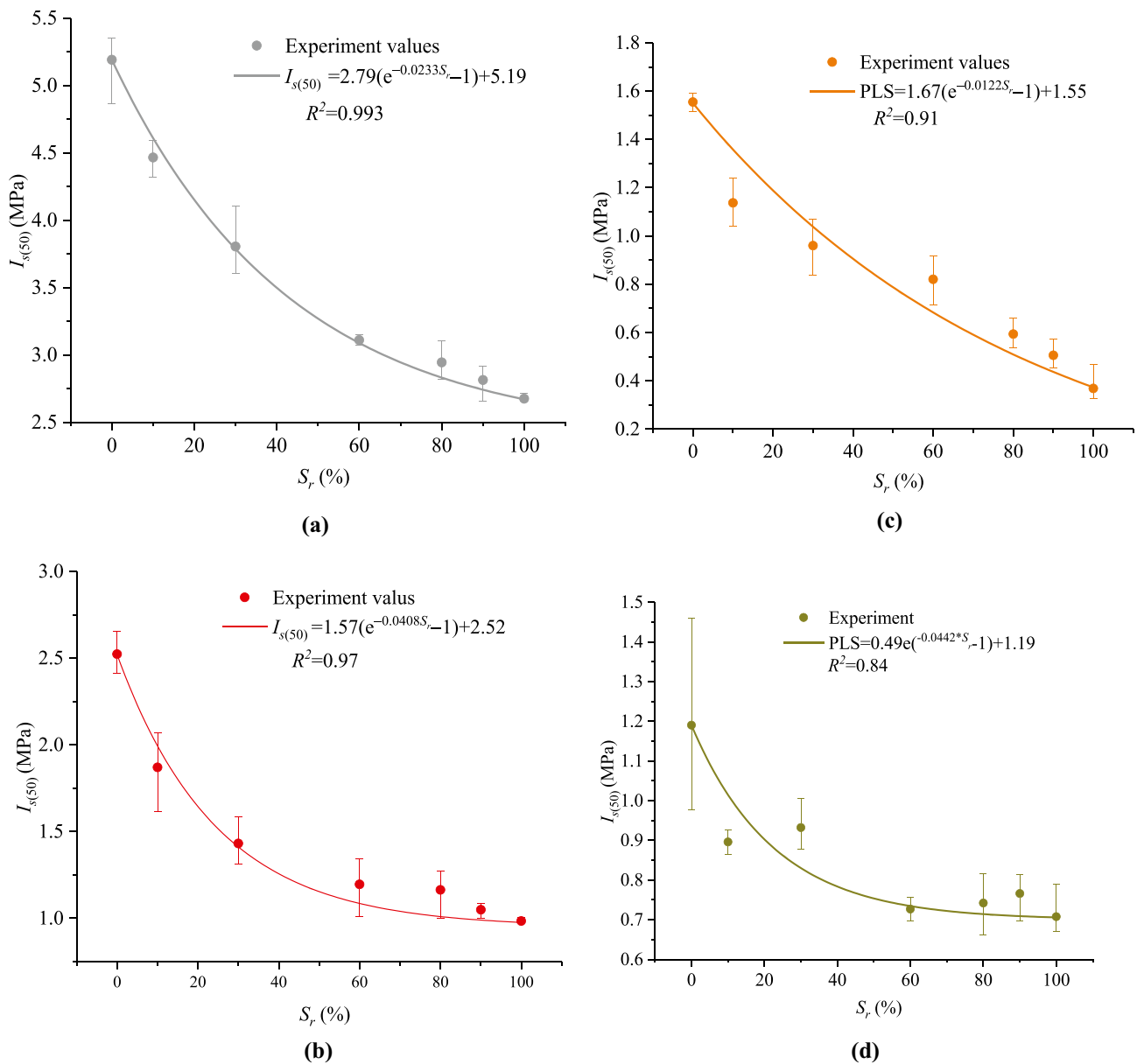
Fig. 10 The influence of water saturations on the PLI of sandstones. **a** Grey sandstone. **b** Red sandstone. **c** Brown sandstone. **d** Yellow sandstone

to water. This means that a small amount of water can cause a great reduction in the UCS values for porous clay-bearing sandstones. However, the impact of the clay mineral content is relatively smaller than that of the porosity and saturated elastic modulus. The UCS values estimated by Eq. (14) are in good agreement with the tested UCS values, as shown in Fig. 14. The prediction errors are less than 10% for all sandstones, although the UCS values of sandstones range from 10 to 130 MPa. Therefore, Eq. (14) is suitable for predicting the UCS values of clay-bearing sandstones with any level of water saturation.

Discussions

The critical water saturation

The strengths of sandstones decrease very quickly at low water saturation levels. The loss rate gradually decreases with increasing water saturation. The strength loss fractions of sandstones against water saturations are plotted in Fig. 15. It can be observed that most of the UCS was lost below 60% water saturation.

The UCS loss fraction derived from Eq. (14) can be expressed as follows:

Fig. 11 The correlation of UCS and BTS with the PLI for sandstones. **a** UCS versus PLI. **b** BTS versus PLI

$y=20.5x$
$R^2=0.94$

(a)

$y=1.32x$
$R^2=0.99$

(b)
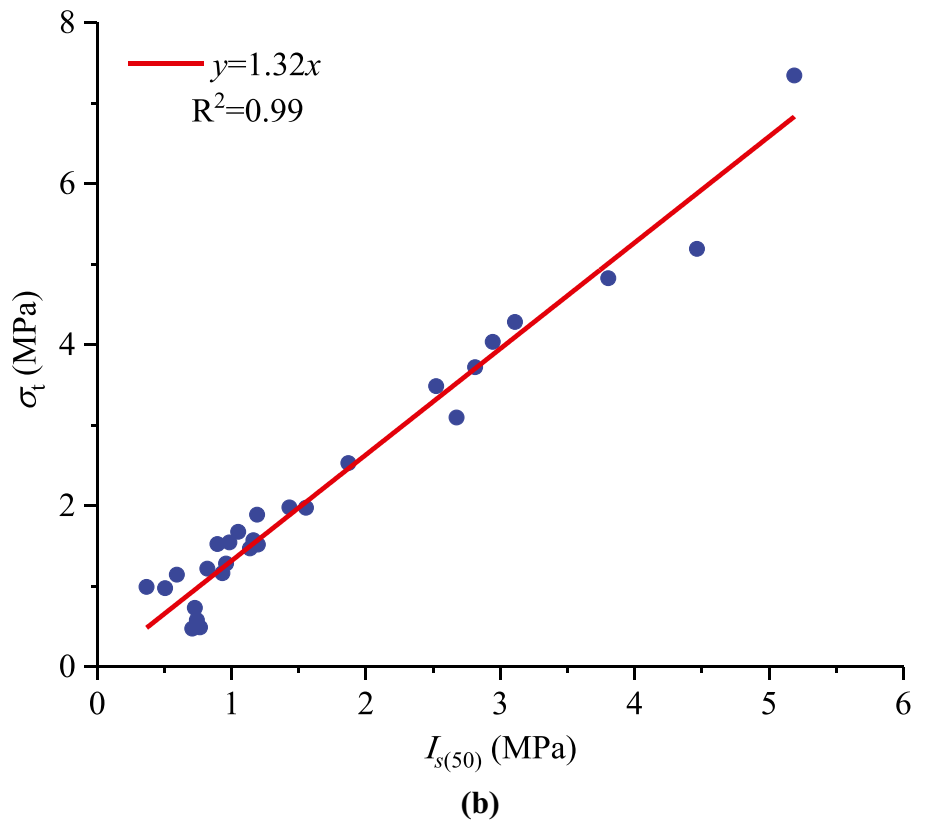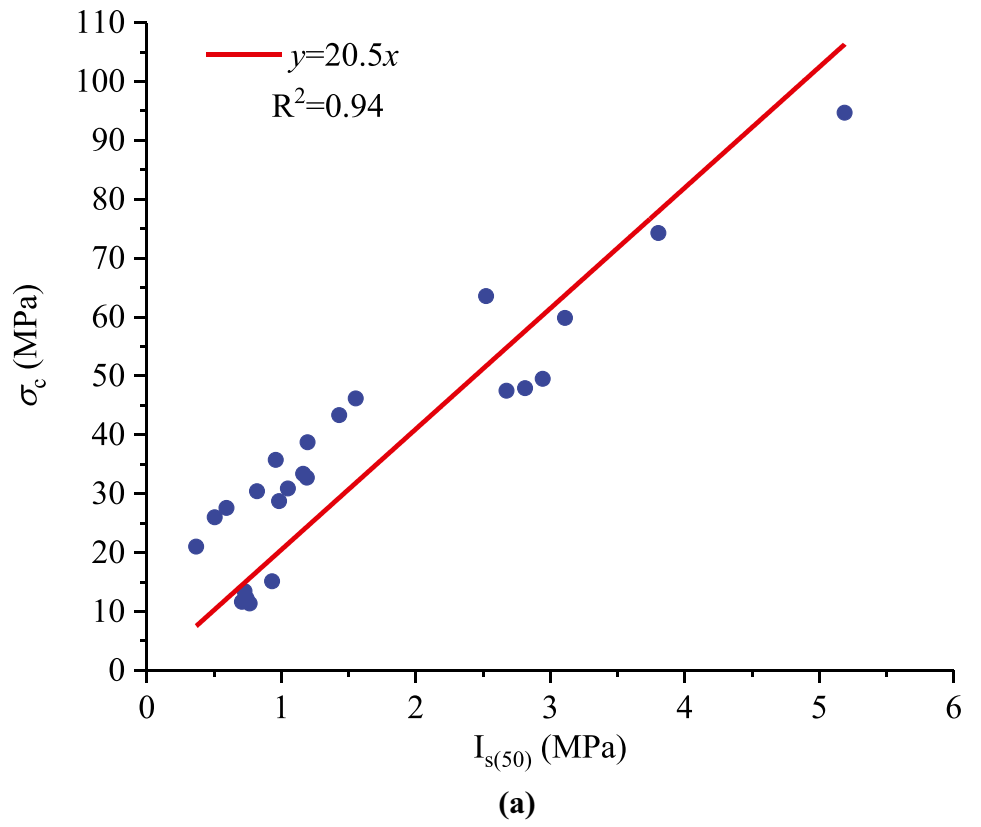
Fig. 12 Determination of *A* in the exponential decay function by fitting 22 sandstones. **a** S1. **b** S2. **c** S3. **d** S4. **e** S5. **f** S6. **g** S7. **h** S8. **i** S9. **j** S10. **k** S11. **l** S12. **m** S13. **n** S14. **o** S15. **p** S16. **q** S17. **r** S18. **s** S19. **t** S20. **u** S21. **v** S22

Fig. 12 (continued)

(i) — Experiment Shao et al. (2010); Fitting curve; Sandstone; A=3.99; R²=0.99

(j) — Experiment Huang et al. (2011,2012); Fitting curve; Siltstone; A=2.33; R²=0.96

(k) — Experiment Zhou et al. (2016); Fitting curve; Sandstone; A=1.61; R²=0.9998

(l) — Experiment Masoumi et al. (2017); Fitting curve; Gosford sandstone; A=2.57; R²=0.91

(m) — Experiment Tang (2018b); Fitting curve; Black sandstone; A=1.87; R²=0.99

(n) — Experiment Tang et al. (2018a); Fitting curve; Red sandstone; A=3.77; R²=0.94

(o) — Experiment Jia et al. (2018,2019); Fitting curve; Siltstone; A=2.21; R²=0.99

(p) — Experiment Wang et al. (2018); Fitting curve; Red sandstone; A=2.28; R²=0.99997
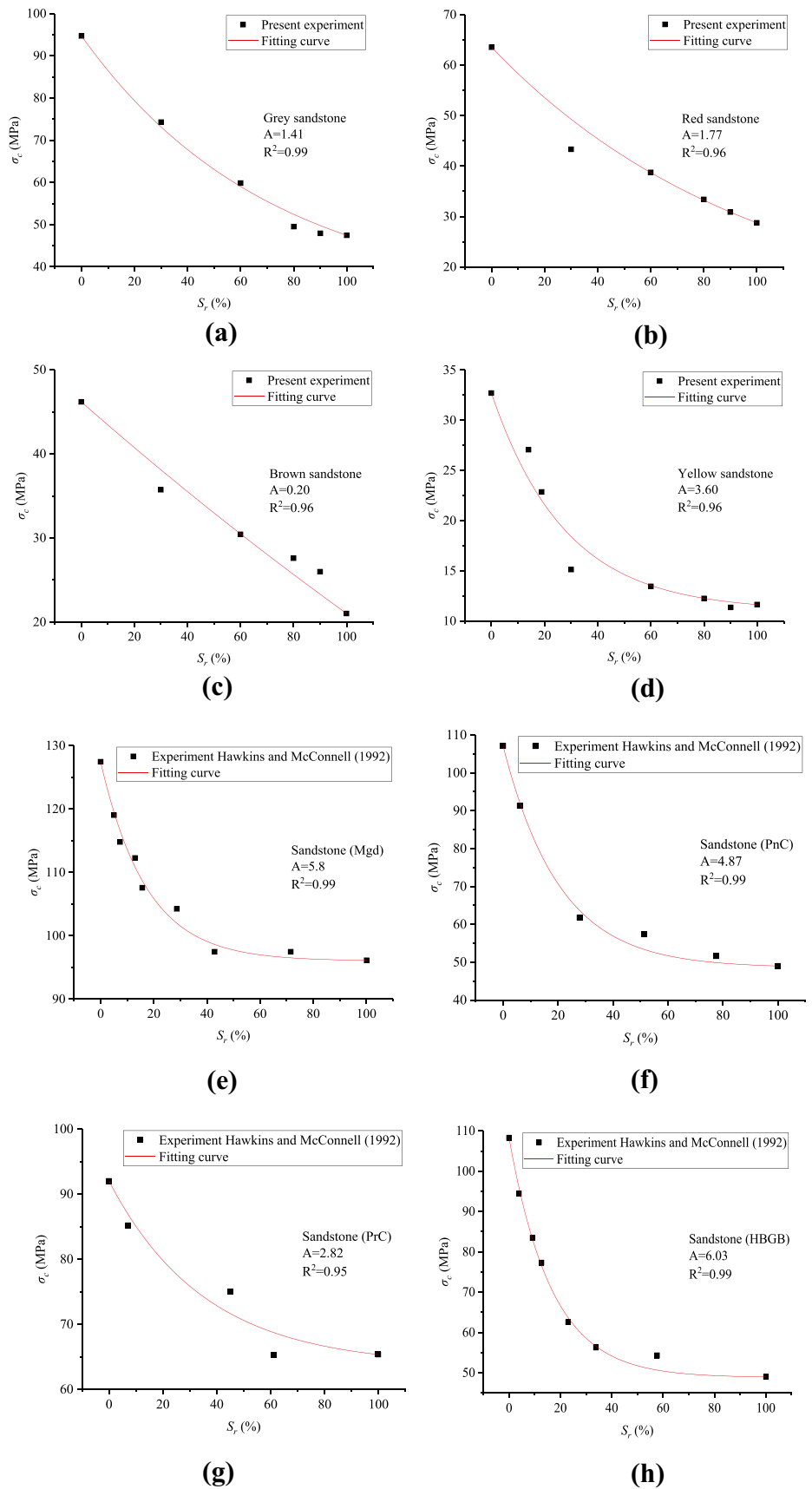
Fig. 12 (continued)

(q)

(r)

(s)

(t)

(u)
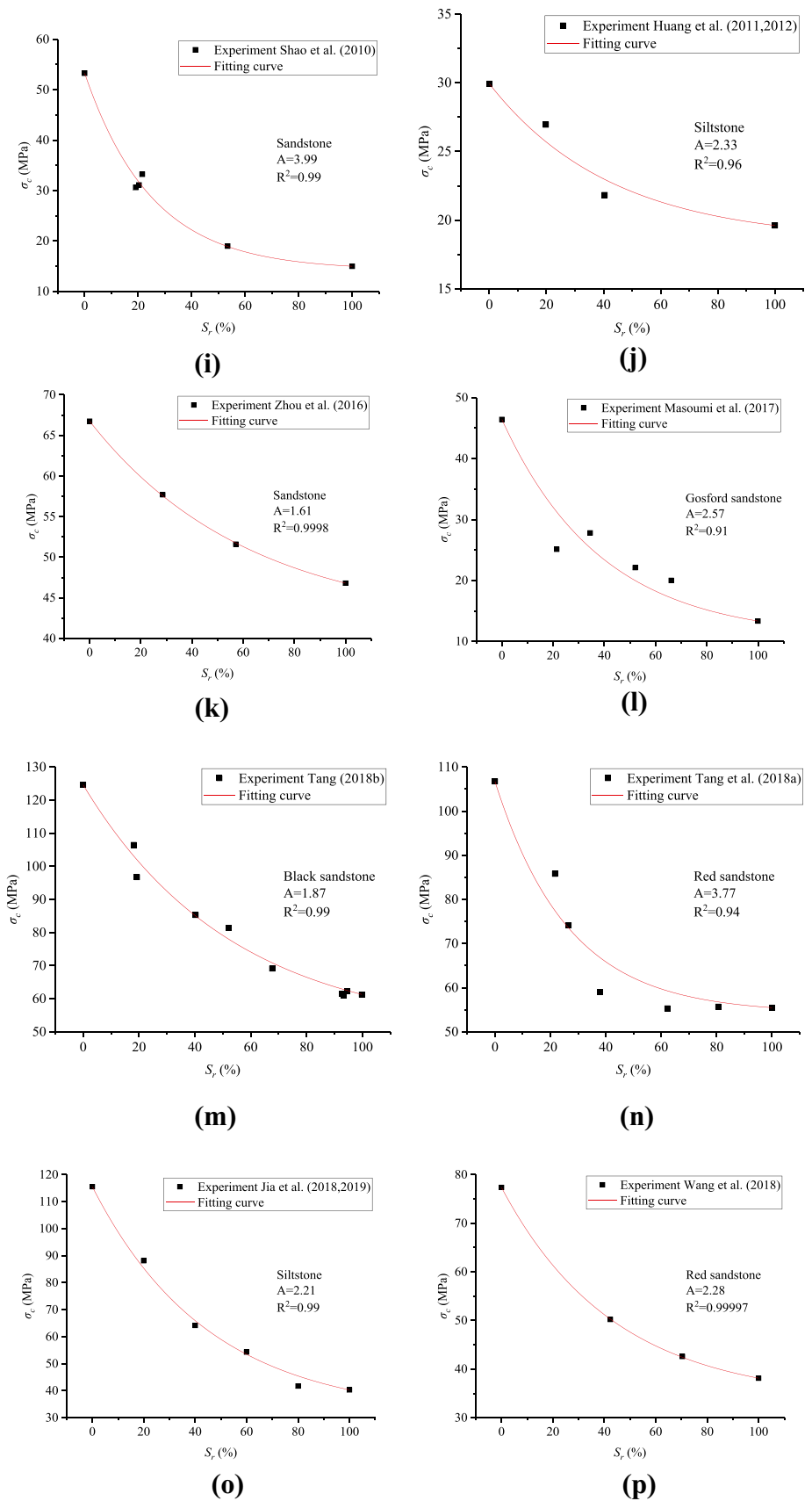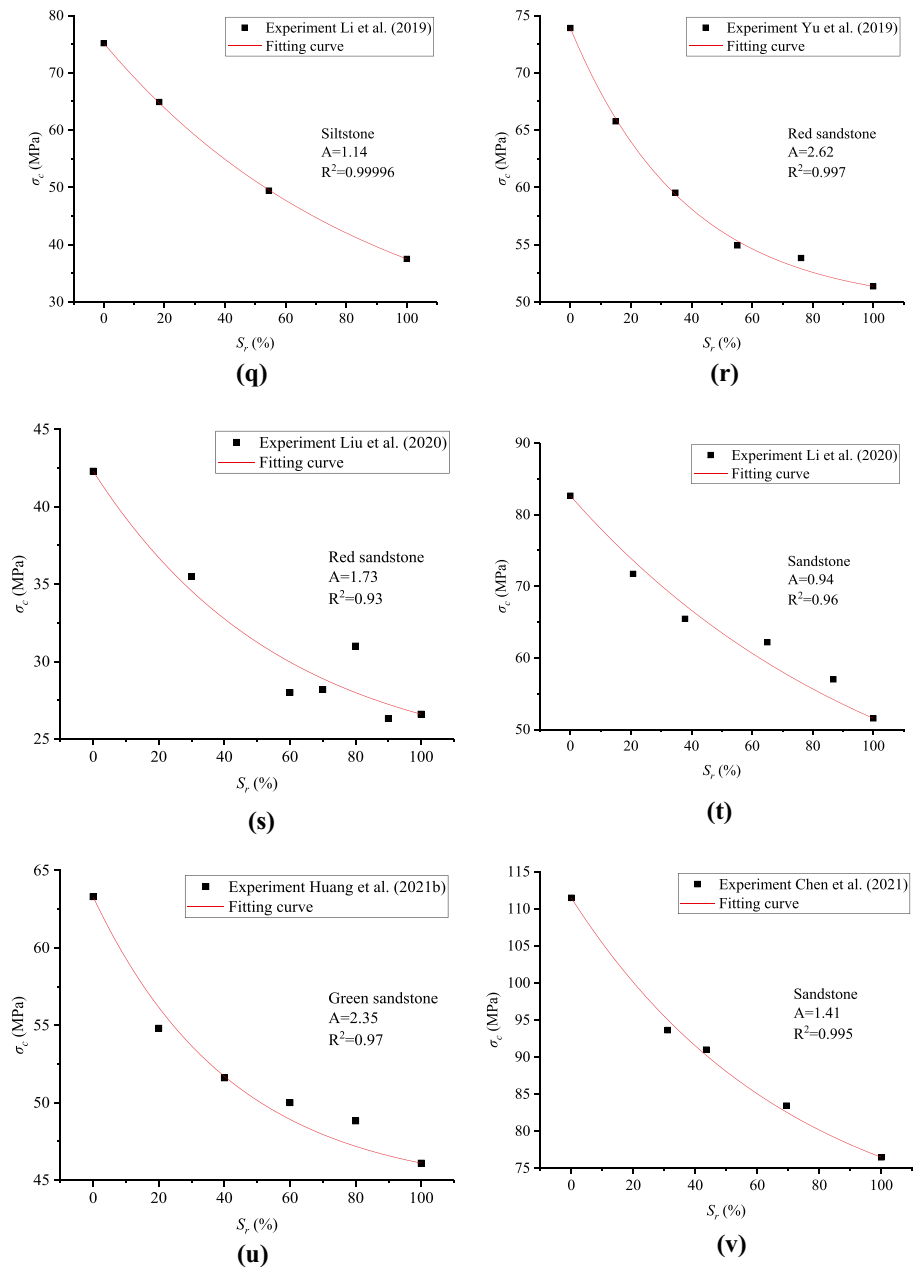
(v)

$$LF = \frac{1}{1 - e^{-A}}(1 - e^{-A \cdot S_r}) \tag{16}$$

In Fig. 15, there is a critical saturation level for the sandstone, beyond which the change in UCS is very small with increasing water saturation. We assume that the UCS loss fraction corresponding to the critical saturation is 90% by considering the measurement error and discreteness of the sandstone samples. Using Eq. (16), the critical saturation levels for a 90% UCS loss have been calculated, which are listed in Table 5. The critical water saturation levels for most

of the sandstones were less than 80%. Nineteen out of 32 sandstones have critical water saturation levels less than 70%. This implies that most sandstones may suffer serious water-weakening damage under natural absorption conditions in engineering fields because the natural water absorption saturation level is generally larger than 70% (Fig. 5). For the PnB sandstone from Hawkins and McConnell (1992), the *LF* value is only 35%. Therefore, a small water saturation level may induce a great UCS loss. The multiple linear regression method given in "A developed prediction model of UCS considering water saturation levels" section was also

Table 2 The common physico-mechanical parameters for sandstones

No.	E_s (GPa)	CM (%)	n (%)	W_f (%)	References
S1	5.39	21.1	4.88	1.76	Present experiment
S2	3.7	10.6	9.95	4.12	Present experiment
S3	2.13	4.6	14.81	6.56	Present experiment
S4	1.03	7.0	20.99	10.39	Present experiment
S5	16.4	74.0	9.5	2.79	Hawkins and McConnell
S6	13.3	43.0	8.51	1.94	(1992)
S7	16.2	0.0	5.6	2.13	
S8	9.0	60	7.05	3.93	
S9	1.3	25.0	33.3	7.84	Shao et al. (2010)
S10	4.24	40.3	9.76	3.74	Huang and Zhang (2011), Huang et al. (2012)
S11	6.25	4.0	9.3	3.5	Zhou et al. (2016)
S12	1.98	13.0	18.0	6.9	Masoumi et al. (2017)
S13	12.24	21.78	4.7	1.74	Tang (2018)
S14	10.93	1.9	11.6	3.35	Tang et al. (2018)
S15	2.56	27.0	7.5	3.02	Jia et al. (2018, 2019)
S16	3.38	3.0	15.8	7.49	Wang et al. (2018) Zheng et al. (2018)
S17	10.6	14.9	6.80	2.79	Li et al. (2019)
S18	8.1	2.0	12.6	4.74	Yu et al. (2019)
S19	3.7	11.24	12.23	5.1	Liu et al. (2020)
S20	7.27	5.6	7.0	2.8	Li et al. (2020)
S21	5.05	14.0	13.0	5.56	Huang et al. (2021b)
S22	14.92	16.5	4.7	3.63	Chen et al. (2021)

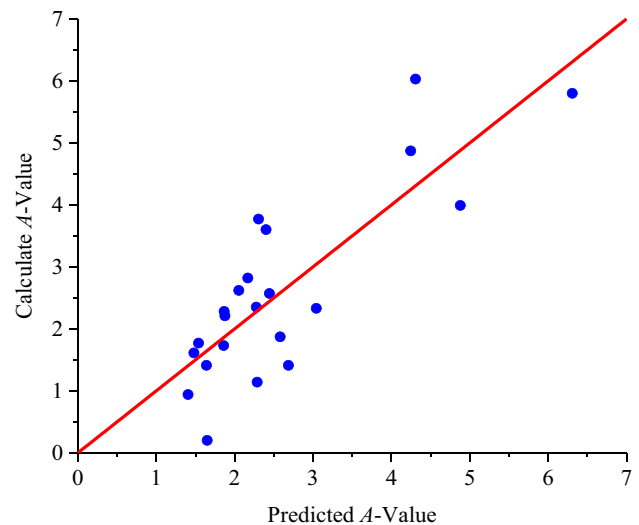**Table 3** Results of the best subset regression

Adjusted R^2 (%)	Mallows' C_p	E_s (GPa)	CM (%)	n (%)	W_a (%)
45.2	11.0	–	√	–	–
5.1	32.2	√	–	–	–
51.8	8.2	–	√	√	–
48.5	9.8	–	√	–	√
62.7	3.7	√	√	√	–
58.9	5.5	√	√	–	√
62.2	5.0	√	√	√	√

Fig. 13 Predicted A values versus measured A values of sandstones

Fig. 14 Predicted UCS versus measured UCS for sandstones

adopted to build the relationship between the critical water saturation levels and the intrinsic properties of 22 sandstones. The predicted function of this critical water saturation level can be expressed as follows:
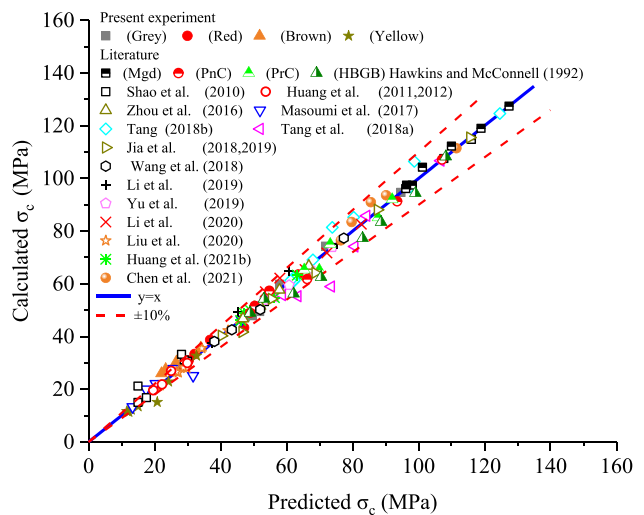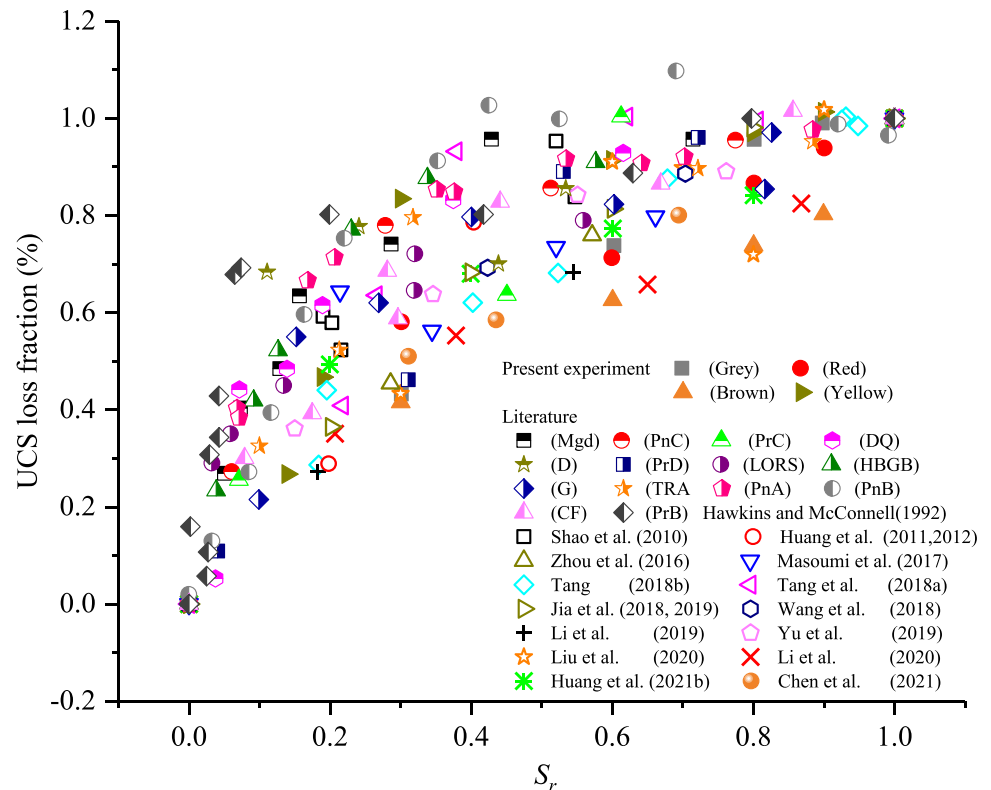
$$S_{rc} = 102.41 - 1.33n(\%) - 1.38E_s(\text{GPa}) - 0.45CM(\%) \tag{17}$$

The calculated values from the experiment are in good agreement with the values predicted by Eq. (17) (Fig. 16). The critical water saturation levels are mainly distributed between 60 and 80%. It can be concluded that sandstones with higher porosity, more clay minerals and larger elastic modulus have lower Src values and are more sensitive to water. Therefore, more attention should be given to high porous sandstone and clay-bearing sandstone when water is available. The previous literature shows that the critical

Table 4 Values of the coefficients from the best subset regression

β_0	β_1	β_2	β_3	F	p	$\hat{R}^2$
−0.743	0.1268	0.1358	0.0489	12.76	0.0001	0.627

Fig. 15 The UCS loss fraction against the water saturation

saturation levels for freeze–thaw deterioration of sandstones is also in the range of 60~80%, and the freeze–thaw action will cause significant damage and strength loss beyond this value (Huang et al. 2018, 2020b, 2020c, 2021a, 2022a). Therefore, water is harmful to sandstones both at normal and low temperatures.

The roles of clay minerals

This study only investigated the influence of water saturation levels on the mechanical strength of sandstones because the water-weakening effect varies greatly among different rock types, and sedimentary rocks usually suffer higher strength loss than igneous and metamorphic rocks. The UCS and elastic modulus losses of different rocks under dry to saturated conditions were comprehensively summarized by Wong et al. (2016). They claimed that the sandstones experienced much more serious water-weakening effects. One important reason may be that the sandstone usually contains some clay minerals. The clay mineral content is an important factor influencing the water-weakening degree because the swelling volume increases with increasing clay mineral content and will induce more serious softening damage. Rocks with higher clay contents have more pores and clay surfaces, which are useful for cation exchange (Lyu et al. 2015). According to Eq. (15), A is positively correlated with the total clay mineral content.

However, the coefficient of the clay mineral item is only 0.0489, which is much smaller than the other two coefficients. The influence of the clay mineral content does not seem to be as great as scholars claim because most sandstones do not contain swelling clay minerals, such as montmorillonite (Table 6). The montmorillonite has the greatest water absorption content and largest expansion of the clay minerals. Therefore, rocks with more expansible clay mineral contents have higher decay rates and obvious microcracks can occur (Zhang et al. 2016). However, sandstones with few expansible minerals do not show obvious damage when soaked in water. Lu et al. (2017) measured the internal structure of mudstone and sandstone after being saturated with water. Clay minerals occupied 57.6% of the volume in the mudstone, including kaolinite, montmorillonite and illite. The sandstone clay mineral content was 21.5%, but montmorillonite was absent. CT technology was adopted to show the microstructures of these two rocks (Fig. 17). Microcracks were only produced in the mudstone in the saturated state. This implies that serious macromicroscopic damage occurs inside the mudstone; however, the water weakening in the sandstone occurs on a much smaller scale, which is difficult to capture by CT. This difference was mainly caused by montmorillonite. Kaolinite and illite are clay minerals with very low expansion levels; therefore, they cannot induce microcracks inside the sandstone after soaking in water. In addition, many previous studies showed

**Table 5** Calculated and measured critical saturations for the sandstones

UCS (%)	S_r (%)	S_{rc} (%)	n (%)	E_s (GPa)	CM (%)	Rock types	References
96	80	81	4.88	5.39	21.1	Grey	Experiment
87	80	78	9.95	3.7	10.6	Red	
74	80	89	14.81	2.13	4.6	Brown	
91	60	58	20.99	1.03	7	Yellow	
96	43	39	9.5	16.4	74	Mgd	Hawkins and McConnell (1992)
96	77	46	8.51	13.3	43	PnC	
100	61	66	5.6	16.2	0	PrC	
93	62	45	1.42	24	/	DQ	
86	53	34	15.75	15.4	/	D	
89	53	72	4.7	33.3	/	PrD	
79	56	54	6.83	26.2	/	LORS	
91	58	38	7.05	9	60	HBGB	
97	83	59	38.6	0.9	/	G	
90	72	55	12.24	5.9	/	TRA	
92	53	37	7.57	12.2	/	PnA	
91	35	41	7.05	15.2	/	PnB	
87	67	61	1.01	19.9		CF	
89	63	20	12.39	7.9	/	PrB	
90	53	54	33.3	1.3	25	Sandstone	Shao et al. (2010)
79	40	72	9.76	4.24	40.3	Siltstone	Huang and Zhang (2011), Huang et al. (2012)
76	57	79	9.3	6.25	4	Sandstone	Zhou et al. (2016)
80	66	69	18	1.98	13	Gosford	Masoumi et al. (2017)
88	68	77	4.7	12.24	21.78	Black	Tang (2018)
93	38	56	11.6	10.93	1.9	Red	Tang et al. (2018)
98	80	73	7.5	2.56	27	siltstone	Jia et al. (2018, 2019)
89	70	72	15.8	3.38	3	Red	Wang et al. (2018) Zheng et al. (2018)
68	54	83	6.8	10.6	14.9	Siltstone	Li et al. (2019)
89	76	69	12.6	8.1	2	Red	Yu et al. (2019)
91	60	78	12.23	3.7	11.24	Red	Liu et al. (2020)
66	65	85	7	7.27	5.6	Sandstone	Li et al. (2020)
84	80	72	13	5.05	14	Green	Huang et al. (2021b)
80	69	81	4.7	14.92	16.5	Sandstone	Chen et al. (2021)

that sandstones containing little expansible clay minerals could recover their strengths after drying, even after having suffered several dry–wet cycles (Zhao et al. 2017; Tang 2018). In contrast, if some montmorillonite or I/M mixed layer (mixed layer of illite and montmorillonite) was contained, the dry–wet damage was irreversible (Hawkins and McConnell 1992).

In this study, the main clay minerals in the sandstones are illite, kaolinite and chlorite. They are typical clay minerals but have very low expansibility. Although the contribution of the clay mineral content to the decay parameter A is smaller than that of the porosity and elastic modulus, the absolute UCS loss under saturated conditions still has a linear increasing trend with the clay mineral content (Fig. 18). Two sandstones do not satisfy this law, including

the siltstone (S10) and Mgd sandstone (S5) according to Huang and Zhang (2011), Huang et al. (2012) and Hawkins and McConnell (1992), respectively. The clay minerals in these sandstones mainly contain nonexpansible illite or kaolinite without any montmorillonite. In addition, the absorption water contents are only 2.79% (S10) and 3.74% (S5) (Table 2). Therefore, the water content is too small to cause a remarkable reduction in the UCS in the absence of montmorillonite. For the siltstone (S15) from Jia et al. (2018, 2019), the UCS loss exceeded 75 MPa, although the clay mineral content was only 27% because it contained approximately 12.96% I/M mixed layer minerals. The sandstone (S13) used by Tang (2018) lost more than 63.4 MPa of its UCS after 100% water saturation because this sandstone contained approximately 0.89% swelling clay minerals. In addition,

Fig. 16 Calculated S_{rc} by experiment versus predicted S_{rc} using linear regression
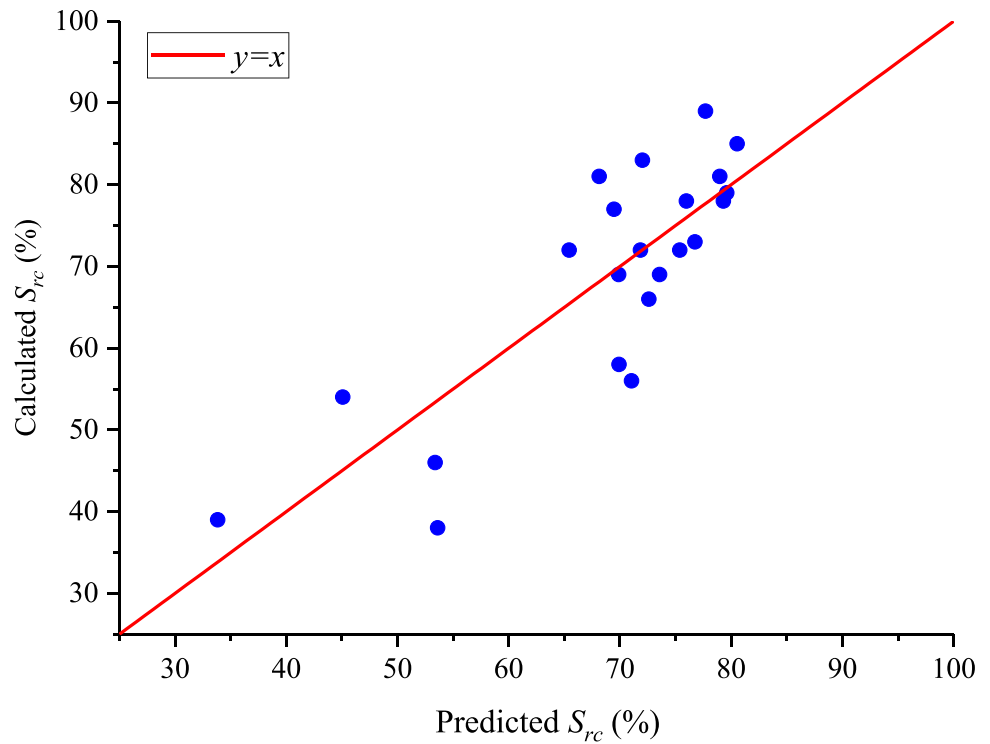

Table 6 The detailed clay mineral content and UCS loss for the sandstones

No.	CM (%)	Ill (%)	Kao (%)	Chl (%)	Mon (%)	I/M (%)	C/M (%)	A	$\sigma_c^D - \sigma_c^S$(MPa)	References
S1	21.1	12.03	/	6.12	/	2.95	/	1.41	47.2	Present experiment
S2	10.6	0.64	8.69	/	/	1.27	/	1.77	34.8	
S3	4.6	1.93	1.56	0.14	/	0.97	/	0.2	25.2	
S4	7.0	0.77	/	0.28	/	/	5.95	3.6	21.1	
S5	74.0	17.5	55	1.5	/	/	/	5.8	31.3	Hawkins and McConnell
S6	43.0	20	20	3	/	/	/	4.87	58.1	(1992)
S7	0.0	0	0	0	/	/	/	2.82	26.7	
S8	60	55	5	0	0	0	0	6.03	59.3	
S9	25.0	/	/	/	/	/	/	3.99	38.3	Shao et al. (2010)
S10	40.3	19.7	/	20.6	/	/	/	2.33	10.3	Huang and Zhang (2011), Huang et al. (2012)
S11	4.0	1	/	2	<1	/	/	1.61	20	Zhou et al. (2016)
S12	13.0	7	6	/	/	/	/	2.57	33.1	Masoumi et al. (2017)
S13	21.78	20.89	/	/	0.89	/	/	1.87	63.4	Tang (2018)
S14	1.9	/	/	/	/	/	/	3.77	51.26	Tang et al. (2018)
S15	27.0	6.21	/	7.83	/	12.96	/	2.21	75.3	Jia et al. (2018, 2019)
S16	3.0	/	/	/	/	/	/	2.28	39.2	Wang et al. (2018) Zheng et al. (2018)
S17	14.9	8.7	6.2	/	/	/	/	1.14	37.7	Li et al. (2019)
S18	2.0	/	/	/	/	/	/	2.62	22.6	Yu et al. (2019)
S19	11.24	7.24	/	4	/	/	/	1.73	15.7	Liu et al. (2020)
S20	5.6	2.51	/	3.09	/	/	/	0.94	31.1	Li et al. (2020)
S21	14.0	2.4	10.5	0.7	/	0.4	/	2.35	17.2	Huang et al. (2021b)
S22	16.5	8.1	6.1	2.3	/	/	/	1.41	35	Chen et al. (2021)

Ill illite, *Kao* kaolinite, *Chl* chlorite, *Mon* montmorillonite, *I/M* mixed-layer of illite/montmorillonites, *C/M* mixed-layer of chlorite/montmorillonites

Fig. 17 Comparison of the water-weakening damage between mudstone and sandstone by CT technology (modified from Lu et al. 2017). **a** Mudstone. **b** Sandstone
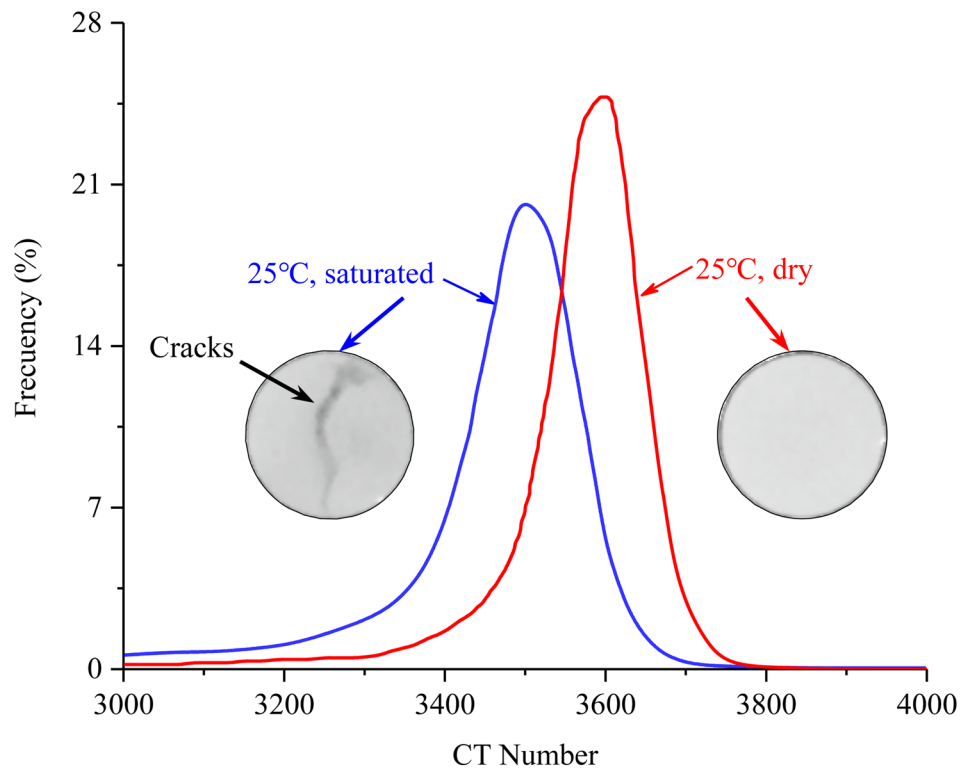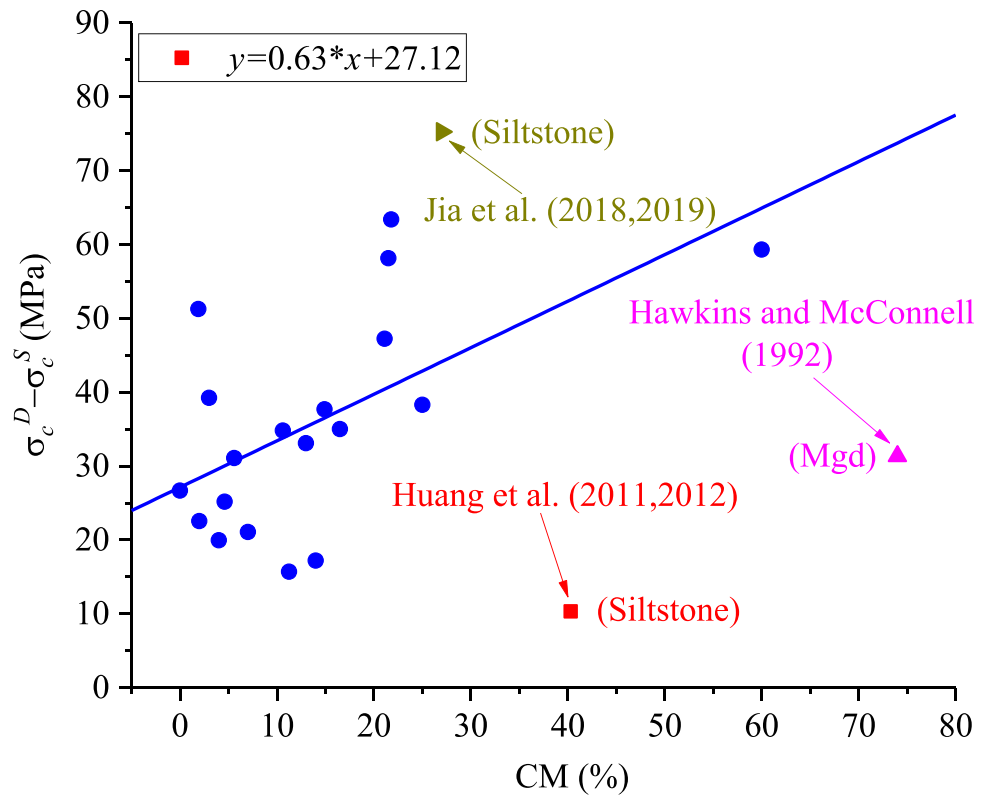

**(a)** Mudstone
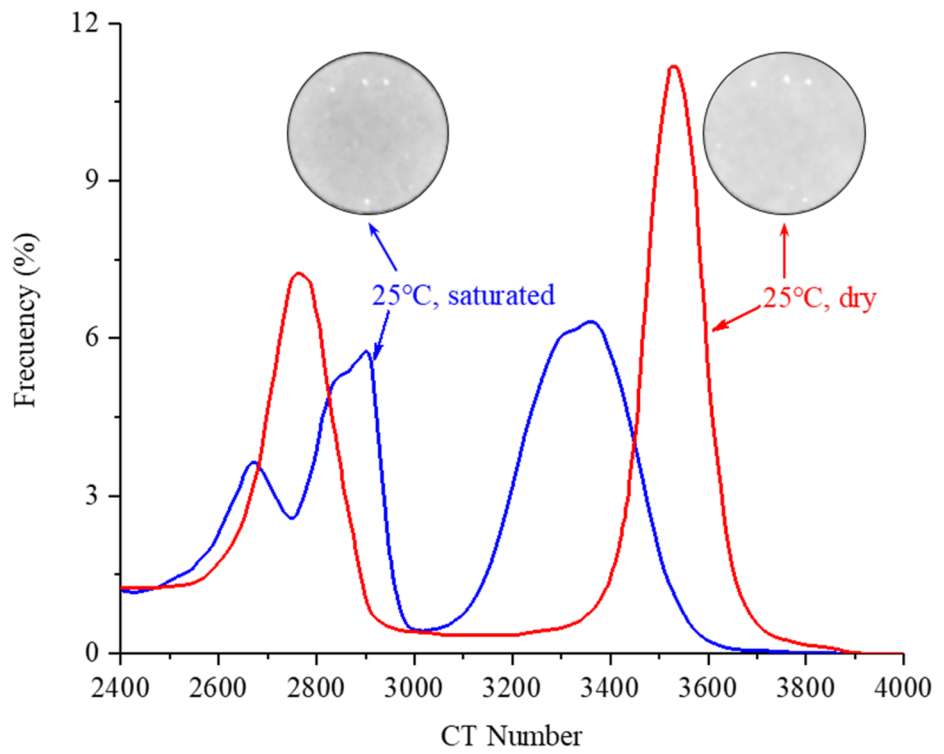
(b) Sandstone

Fig. 18 The UCS loss of 22 sandstones after completely saturated against clay mineral content

sandstones (S1~S3) lost most of their UCS after reaching full saturation even though their initial UCS values were not high. As a result, it can be concluded that the influence of swelling clay minerals, such as montmorillonite, plays a much more important role in the water-weakening effect of sandstones.
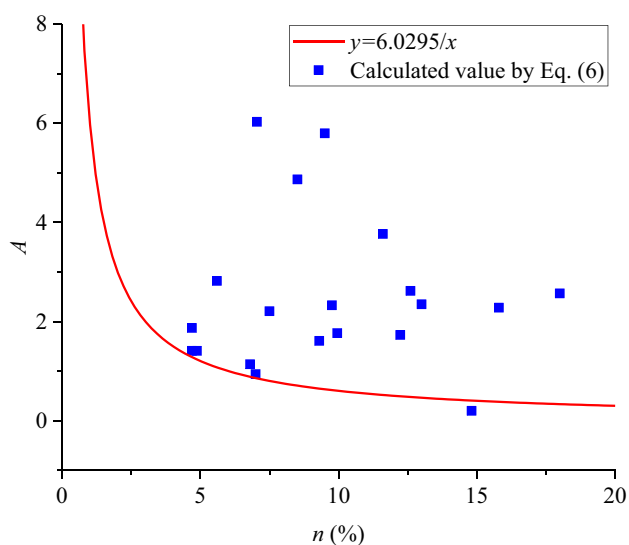
Fig. 19 Relationship between the UCS and the elastic modulus for these sandstones
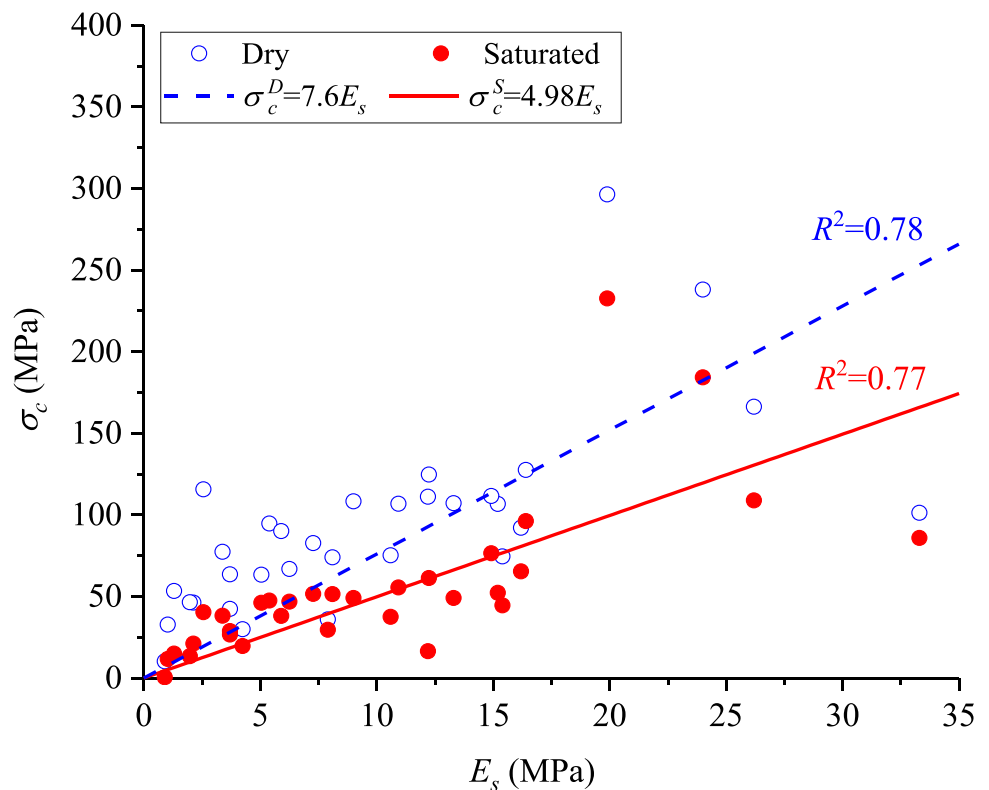
Effect of the elastic modulus and porosity

Hard sandstones seem to be more sensitive to water because a sandstone with a higher elastic modulus will produce a larger value of A and, thus, cause the UCS to decrease more quickly against increasing water saturation levels. Hawkins and McConnell (1992) also held the view that weaker sandstones were more sensitive to moisture content, which was not supported by the experiment. Sandstone with a larger elastic modulus usually has a larger UCS (Fig. 19). Therefore, hard sandstones with large elastic modulus values descend more and faster when soaked in water, such as sandstones S5, S6, S8, S13 and S14.

Vásárhelyi and Ván (2006) claimed that the material parameter in Eq. (6) was inversely related to porosity, which could be expressed as $A = 6.0295 / n$. This relationship was further investigated by using the calculated values of A for the above 22 sandstones. Figure 20 shows that this empirical function may not be suitable for sandstones. Therefore, multivariate linear regression was used to predict the value of A by adopting porosity, elastic modulus and clay mineral content as the input variables. The multivariate linear regression function illustrates that the value of A is linearly positively correlated with porosity, which is in conflict with Eq. (7) in (Vásárhelyi and Ván 2006). Sandstone with high porosity can absorb much more water, which can provide more void space for water–rock action. The adverse influence of porosity on the strength caused by water-weakening effects in this study is in accordance with the literature (Wong et al. 2016), in which a negative power relationship was observed between the UCS and porosity. Some other potential internal and external factors influencing the water-weakening effects

can also be found in the review (Wong et al. 2016). Nevertheless, a novel finding in this study is that the relationship between the UCS loss caused by water saturation and the initial internal properties of sandstones (clay mineral content, elastic modulus and porosity) is quantified.

Conclusions

The strength loss of four typical sandstones is investigated experimentally. The UCS, PLI and BTS values decrease quickly with increasing water saturation levels, especially when the water saturation level increases from 0 to 60%. By comparison, both the exponential decay function and logarithmic decay function can be used to predict the strength loss under any water saturation.

To further investigate the correction of the intrinsic properties of sandstones with the water-weakening degree, multiple linear regression analysis is conducted. The UCS loss caused by water saturation is related to the porosity, elastic modulus and clay mineral content. Sandstone with high porosity, a large elastic modulus and large clay mineral content experiences more and faster UCS loss when in contact with water. The other potential factors influencing the water-weakening effects on rocks need to be researched in the future.

A critical saturation level corresponding to the 90% UCS loss is proposed in this study. The critical saturation values for most sandstones are in the range of 60~80%, beyond which the UCS loss caused by the increased water saturation is very small. Sandstone with high porosity, a large elastic modulus and a large clay mineral content has a smaller critical saturation value, which is more sensitive to water.

The clay minerals in these sandstones mainly include illite, kaolinite and chlorite, which have low swelling abilities. Therefore, the influence of the clay mineral content on the water weakening of sandstones is not remarkable if highly expansible clay minerals are absent. Highly expansible clay minerals play an important role in the water weakening of sandstones.

Declarations

Conflict of interest The authors declare no competing interests.

Fig. 20 The values of material parameter A versus porosity for 22 sandstones

References

ASTM (2008a) ASTM D3967-08 Standard test method for splitting tensile strength on intact rock core specimens

ASTM (2008b) ASTM D4543–08 Standard practices for preparing rock core as cylindrical test specimens and verifying conformance to dimensional and shape tolerances

ASTM (2008c) ASTM D5731–08 Standard test method for determination of the point load strength index of rock and application to rock strength classifications

ASTM (2010) ASTM D7012-10 Standard test method for compressive strength and elastic moduli of intact rock core specimens under varying states of stress and temperatures

Chen G, Li T, Wei W, Zhu Z (2019) Weakening effects of the presence of water on the brittleness of hard sandstone. B Eng Geol Environ 78:1471–1483. https://doi.org/10.1007/s10064-017-1184-3

Chen L, Jian Z, Zheng Z (2017) Acoustic emission characteristics of compressive deformation and failure of siltstone under different water contents. Adv Mater Sci Eng ID:4035487. https://doi.org/10.1155/2017/4035487

Chen PZ, Tang SB, Liang X, Zhang YJ, Tang CA (2021) The influence of immersed water level on the short- and long-term mechanical behavior of sandstone. Int J Rock Mech Min Sci 138:104631. https://doi.org/10.1016/j.ijrmms.2021.104631

Cherblanc F, Berthonneau J, Bromblet P, Huon V (2016) Influence of water content on the mechanical behaviour of limestone: role of the clay minerals content. Rock Mech Rock Eng 49:2033–2042. https://doi.org/10.1007/s00603-015-0911-y

Erguler ZA, Ulusay R (2009) Water-induced variations in mechanical properties of clay-bearing rocks. Int J Rock Mech Min Sci 46(2):355–370. https://doi.org/10.1016/j.ijrmms.2008.07.002

Hawkins AB, McConnell BJ (1992) Sensitivity of sandstone strength and deformability to changes in moisture content. Q J Eng Geol Hydrogeol 25(2):115–130. https://doi.org/10.1144/GSL.QJEG.1992.025.02.05

Heidari M, Khanlari GR, Kaveh MT, Kargarian S (2012) Predicting the uniaxial compressive and tensile strengths of gypsum rock by point load testing. Rock Mech Rock Eng 45:265–273. https://doi.org/10.1007/s00603-011-0196-8

He W, Chen K, Hayatdavoudi A, Sawant K, Lomas M (2019) Effects of clay content, cement and mineral composition characteristics on sandstone rock strength and deformability behaviors. J Pet Sci Eng 176:962–969. https://doi.org/10.1016/j.petrol.2019.02.016

Huang M, Liu XR, Deng T (2012) Study on the creep properties of T_2b^2 siltite in terms of the damage law induced by water. J Fuzhou Univ (Nat Sci Ed) 40(3):399–405 (In Chinese)

Huang M, Zhang XD (2011) Test study on the creep properties of T_2b^2 siltite in different moisture states. Ind Constr 41(1):77–85. https://doi.org/10.13204/j.gyjz201101019. (In Chinese)

Huang SB, Cai C, Yu SL, He YB, Cui XZ (2022a) Study on damage evaluation indexes and evolution models of rocks under freeze-thaw considering the effect of water saturations. Int J Damage Mech. https://doi.org/10.1177/10567895221106241

Huang SB, Cai YT, Liu YZ, Liu GF (2021a) Experimental and theoretical study on frost deformation and damage of red sandstones with different water contents. Rock Mech Rock Eng 54:4163–4181. https://doi.org/10.1007/s00603-021-02509-9

Huang SB, He YB, Liu GF, Lu ZX, Xin ZK (2020a) Effect of water content on the mechanical properties and deformation characteristics of the clay-bearing red sandstone. B Eng Geol Environ 80:1767–1790. https://doi.org/10.1007/s10064-020-01994-6

Huang SB, He YB, Liu XW, Xin ZK (2021b) Experimental investigation of the influence of dry-wet, freeze-thaw and water immersion treatments on the mechanical strength of the clay-bearing green sandstone. Int J Rock Mech Min Sci 138:104613. https://doi.org/10.1016/j.ijrmms.2021.104613

Huang SB, He YB, Yu SL, Cai C (2022b) Experimental investigation and prediction model for UCS loss of unsaturated sandstones under freeze-thaw action. Int J Min Sci Techno 32:41–49. https://doi.org/10.1016/j.ijmst.2021.10.012

Huang SB, Liu QS, Cheng AP, Liu YZ (2018) A statistical damage constitutive model under freeze-thaw and loading for rock and its engineering application. Cold Reg Sci Technol 145:142–150. https://doi.org/10.1016/j.coldregions.2017.10.015

Huang SB, Lu ZX, Ye ZY, Xin ZK (2020b) An elastoplastic model of frost deformation for the porous rock under freeze-thaw. Eng Geol 278:105820. https://doi.org/10.1016/j.enggeo.2020.105820

Huang SB, Ye YH, Cui XZ, Chen AP, Liu GF (2020c) Theoretical and experimental study of the frost heaving characteristics of the saturated sandstone under low temperature. Cold Reg Sci Technol 174:103036. https://doi.org/10.1016/j.coldregions.2020.103036

Huang SB, Yu SL, Ye YH, Ye ZY, Cheng AP (2022c) Pore structure change and physico-mechanical properties deterioration of sandstone suffering freeze-thaw actions. Constr Build Mater 330:127200. https://doi.org/10.1016/j.conbuildmat.2022.127200

ISRM (1985) Suggested method for determining point load strength: ISRM Commission on testing methods. Int J Rock Mech Min Sci 22(2):51–60. https://doi.org/10.1016/0148-9062(85)92985-7

Jia HL, Wang T, Xiang W, Tan L, Shen YJ, Yang GS (2018) Influence of water content on the physical and mechanical behaviour of argillaceous siltstone and some microscopic explanations. Chin J Rock Mech Eng 37(7):1618–1628. https://doi.org/10.13722/j.cnki.jrme.2017.1037. (In Chinese)

Jia HL, Zi F, Yang GS, Li GY, Shen YJ, Sun Q, Yang PY (2019) Influence of pore water (ice) content on the strength and deformability of frozen argillaceous siltstone. Rock Mech Rock Eng 53:967–974. https://doi.org/10.1007/s00603-019-01943-0

Kahraman S, Gunaydin O (2009) The effect of rock classes on the relation between uniaxial compressive strength and point load index. B Eng Geol Environ 68:345–353. https://doi.org/10.1007/s10064-009-0195-0

Kim E, Changani H (2016) Effect of water saturation and loading rate on the mechanical properties of red and buff sandstones. Int J Rock Mech Min Sci 88:23–28. https://doi.org/10.1016/j.ijrmms.2016.07.005

Kim E, Stine MA, Oliveira DBMD, Changani H (2017) Correlations between the physical and mechanical properties of sandstones with changes of water content and loading rates. Int J Rock Mech Min Sci 100:255–262. https://doi.org/10.1016/j.ijrmms.2017.11.005

Li BY, Liu J, Bian K, Ai F (2019) Experimental study on the mechanical properties weakening mechanism of siltstone with different water content. Arabian J Geosci 12:656. https://doi.org/10.1007/s12517-019-4852-8

Li K, Li M, Zhang D, Liu CX, Ma D (2020) Effect of moisture content on bursting liability of sandstone due to freeze-thaw action. Shock Vib ID:8832528. https://doi.org/10.1155/2020/8832528

Liu YZ, Cai YT, Huang SB, Guo YL, Liu GF (2020) Effect of water saturation on uniaxial compressive strength and damage degree of clay-bearing sandstone under freeze-thaw. B Eng Geol Environ 79:2021–2036. https://doi.org/10.1007/s10064-019-01686-w

Li XS, Peng K, Peng J, Hou D (2021) Experimental investigation of cyclic wetting-drying effect on mechanical behavior of a medium-grained sandstone. Eng Geol 293:106335. https://doi.org/10.1016/j.enggeo.2021.106335

Lu YL, Wang LG, Sun XK, Wang J (2017) Experimental study of the influence of water and temperature on the mechanical behavior of mudstone and sandstone. B Eng Geol Environ 76:645–660. https://doi.org/10.1007/s10064-016-0851-0

Lyu Q, Ranjith PG, Long XP, Kang Y, Huang M (2015) A review of shale swelling by water adsorption. J Nat Gas Sci Eng 27:1421–1431. https://doi.org/10.1016/j.jngse.2015.10.004

Masoumi H, Horne J, Timms W (2017) Establishing empirical relationships for the effects of water content on the mechanical behavior of Gosford sandstone. Rock Mech Rock Eng 50:2235–2242. https://doi.org/10.1007/s00603-017-1243-x

Palchik V (1999) Influence of porosity and elastic modulus on uniaxial compressive strength in soft brittle porous sandstones. Rock Mech Rock Eng 32(4):303–309. https://doi.org/10.1007/s006030050050

Ruedrich J, Bartelsen T, Dohrmann R, Siegesmund S (2011) Moisture expansion as a deterioration factor for sandstone used in buildings. Environ Geol 63:1545–1564. https://doi.org/10.1007/s12665-010-0767-0

Shao MS, Li L, Li ZX (2010) Elastic wave velocity and mechanical properties of sandstone under different water contents at longyou grottoes. Chin J Rock Mech Eng 29(2):3514–3518 (In Chinese)

Shi XC, Cai WQ, Meng YF, Li G (2016) Weakening laws of rock uniaxial compressive strength with consideration of water content and rock porosity. Arabian J Geosci 9(5):369. https://doi.org/10.1007/s12517-016-2426-6

Sun Q, Zhang YL (2019) Combined effects of salt, cyclic wetting and drying cycles on the physical and mechanical properties of sandstone. Eng Geol 248:70–79. https://doi.org/10.1016/j.enggeo.2018.11.009

Tang SB (2018) The effects of water on the strength of black sandstone in a brittle regime. Eng Geol 239:167–178. https://doi.org/10.1016/j.enggeo.2018.03.025

Tang SB, Yu CY, Heap MJ, Chen PZ (2018) The influence of water saturation on the short- and long-term mechanical behavior of red sandstone. Rock Mech Rock Eng 51:2669–2687. https://doi.org/10.1007/s00603-018-1492-3

Vásárhelyi B (2003) Some observations regarding the strength and deformability of sandstones in dry and saturated conditions. B Eng Geol Environ 62:245–249. https://doi.org/10.1007/s10064-002-0186-x

Vásárhelyi B, Ván P (2006) Influence of water content on the strength of rock. Eng Geol 84(1–2):70–74. https://doi.org/10.1016/j.enggeo.2005.11.011

Wang P, Xu JY, Fang XY, Wang PX, Liu SH, Wang HY (2018) Water softening and freeze-thaw cycling induced decay of red-sandstone. Rock Soil Mech 39(6):2065–2072. https://doi.org/10.16285/j.rsm.2016.2098. (In Chinese)

Wasantha PLP, Ranjith PG (2014) Water-weakening behavior of Hawkesbury sandstone in brittle regime. Eng Geol 178:91–101. https://doi.org/10.1016/j.enggeo.2014.05.015

Wasantha PLP, Ranjith PG, Permata G, Bing D (2018) Damage evolution and deformation behaviour of dry and saturated sandstones: Insights gleaned from optical measurements. Measurement 130:8–17. https://doi.org/10.1016/j.measurement.2018.07.075

Wong LNY, Maruvanchery V, Liu G (2016) Water effects on rock strength and stiffness degradation. Acta Geotech 11:713–737. https://doi.org/10.1007/s11440-015-0407-7

Yu C, Tang SB, Tang CA, Duan D, ZhangYJ LZZ, Ma K, Ma TH (2019) The effect of water on the creep behavior of red sandstone. Eng Geol 253:64–74. https://doi.org/10.1016/j.enggeo.2019.03.016

Zeng L, Wang LS, Xu HX, Jiao GN, Cui SN, Han H, Zhang BS (2010) SY/T 5163–2010 Analysis method for clay minerals and ordinary non-clay minerals in sedimentary rocks by the X-Ray diffraction. Petroleum Industry Publishing House, Beijing, China (In Chinese)

Zhang D, Chen AQ, Wang XM, Yan BG, Shi LT, Liu GC (2016) A quantitative determination of the effect of moisture on purple mudstone decay in Southwestern China. CATENA 139:28–31. https://doi.org/10.1016/j.catena.2015.12.003

Zhao ZH, Yang J, Zhang DF, Peng H (2017) Effects of wetting and cyclic wetting–drying on tensile strength of sandstone with a low clay mineral content. Rock Mech Rock Eng 50:485–491. https://doi.org/10.1007/s00603-016-1087-9

Zheng GH, Xu JY, Wang P, Fang XY, Wang PX, Wen M (2018) Static constitutive relation and dynamic mechanical properties of red sandstone with different water saturation. J Vib Shock 37(16):31–37. https://doi.org/10.13465/j.cnki.jvs.2018.16.005. (In Chinese)

Zhou ZL, Cai X, Cao WZ, Li XB (2016) Influence of water content on mechanical properties of rock in both saturation and drying processes. Rock Mech Rock Eng 49:3009–3025. https://doi.org/10.1007/s00603-016-0987-z